

Contents lists available at ScienceDirect

Physics Letters B

www.elsevier.com/locate/physletb

Measurement of the $t\bar{t}$ production cross-section using $e\mu$ events with b -tagged jets in pp collisions at $\sqrt{s} = 13$ TeV with the ATLAS detector

The ATLAS Collaboration*



ARTICLE INFO

Article history:

Received 9 June 2016

Received in revised form 10 August 2016

Accepted 10 August 2016

Available online 16 August 2016

Editor: W.-D. Schlatter

ABSTRACT

This paper describes a measurement of the inclusive top quark pair production cross-section ($\sigma_{t\bar{t}}$) with a data sample of 3.2 fb^{-1} of proton–proton collisions at a centre-of-mass energy of $\sqrt{s} = 13$ TeV, collected in 2015 by the ATLAS detector at the LHC. This measurement uses events with an opposite-charge electron–muon pair in the final state. Jets containing b -quarks are tagged using an algorithm based on track impact parameters and reconstructed secondary vertices. The numbers of events with exactly one and exactly two b -tagged jets are counted and used to determine simultaneously $\sigma_{t\bar{t}}$ and the efficiency to reconstruct and b -tag a jet from a top quark decay, thereby minimising the associated systematic uncertainties. The cross-section is measured to be:

$$\sigma_{t\bar{t}} = 818 \pm 8 \text{ (stat)} \pm 27 \text{ (syst)} \pm 19 \text{ (lumi)} \pm 12 \text{ (beam)} \text{ pb},$$

where the four uncertainties arise from data statistics, experimental and theoretical systematic effects, the integrated luminosity and the LHC beam energy, giving a total relative uncertainty of 4.4%. The result is consistent with theoretical QCD calculations at next-to-next-to-leading order. A fiducial measurement corresponding to the experimental acceptance of the leptons is also presented.

© 2016 The Author(s). Published by Elsevier B.V. This is an open access article under the CC BY license (<http://creativecommons.org/licenses/by/4.0/>). Funded by SCOAP³.

1. Introduction

The top quark is the heaviest known fundamental particle, with a mass m_t which is much larger than any of the other quarks, and close to the scale of electroweak symmetry breaking. The study of its production and decay properties forms a core part of the LHC physics programme. At the LHC, top quarks are primarily produced in quark–antiquark pairs ($t\bar{t}$), and the precise prediction of the corresponding inclusive cross-section is sensitive to the gluon parton distribution function (PDF) and the top quark mass, and presents a substantial challenge for QCD calculational techniques. Physics beyond the Standard Model may also lead to an enhancement of the $t\bar{t}$ production rate.

Calculations of the $t\bar{t}$ production cross-section at hadron colliders are available at full next-to-next-to-leading-order (NNLO) accuracy in the strong coupling constant α_s , including the resummation of next-to-next-to-leading logarithmic (NNLL) soft gluon terms [1–5]. In this paper a reference value of 832^{+40}_{-46} pb at a centre-of-mass energy of $\sqrt{s} = 13$ TeV assuming $m_t = 172.5$ GeV is used, corresponding to a relative precision of $^{+4.8}_{-5.5}\%$. This value was calculated using the `top++ 2.0` program [6]. The combined

PDF and α_s uncertainties of ± 35 pb were calculated using the PDF4LHC prescription [7] with the MSTW2008 68% CL NNLO [8,9], CT10 NNLO [10,11] and NNPDF2.3 5f FFN [12] PDF sets, and added in quadrature to the factorisation and renormalisation scale uncertainty of $^{+20}_{-29}$ pb. The cross-section at $\sqrt{s} = 13$ TeV is predicted to be 3.3 times larger than the cross-section at $\sqrt{s} = 8$ TeV.

Measurements of $\sigma_{t\bar{t}}$ have been made at $\sqrt{s} = 7$ and 8 TeV by both ATLAS [13–15] and CMS [16–18]. The most precise ATLAS measurements of $\sigma_{t\bar{t}}$ at these collision energies were made using events with an opposite-charge isolated electron and muon pair and additional b -tagged jets [13]. This paper documents a measurement of $\sigma_{t\bar{t}}$ at $\sqrt{s} = 13$ TeV using the same final state and analysis technique. Wherever possible, the analysis builds on the studies and procedures used in the earlier publication [13]. A fiducial measurement determining the cross-section in the region corresponding to the experimental lepton acceptance is also presented.

The data and Monte Carlo simulation samples are described in Section 2, followed by the object and event selection in Section 3 and the method for determining the $t\bar{t}$ cross-section in Section 4. The evaluation of backgrounds is discussed in Section 5 and the systematic uncertainties in Section 6. Finally, the results and conclusions are given in Section 7.

* E-mail address: atlas.publications@cern.ch.

Table 1

Summary of Monte Carlo samples used to model the signal and background processes. The ‘Calculation’ column corresponds to the order of the matrix element calculation in the Monte Carlo generator.

Process	Generator + parton shower	Calculation
$t\bar{t}$	POWHEG-Box v2 + PYTHIA6	
	POWHEG-Box v2 + HERWIG++	NLO
	MADGRAPH5_AMC@NLO + HERWIG++	
Wt single top	POWHEG-Box v1 + PYTHIA6	NLO
	POWHEG-Box v1 + HERWIG++	
Z + jets	SHERPA 2.1.1	NLO (up to two partons)
Diboson	SHERPA 2.1.1	NLO (up to two partons)
	POWHEG + PYTHIA8	NLO
t -channel single top	POWHEG-Box v1 + PYTHIA6	NLO
W + jets	POWHEG-Box v2 + PYTHIA8	NLO
$t\bar{t}$ + W/Z	MADGRAPH + PYTHIA8	LO

2. Data and simulation samples

The analysis is performed using the full 2015 proton–proton (pp) collision data sample at $\sqrt{s} = 13$ TeV with 25 ns bunch spacing recorded by the ATLAS detector [19,20]. The data correspond to an integrated luminosity of 3.2 fb^{-1} after requiring stable LHC beams and that all detector subsystems were operational. Events are required to pass either a single-electron or single-muon trigger, with thresholds set to be almost fully efficient for leptons with transverse momentum $p_T > 25$ GeV passing offline selections. Each event includes the signals from on average about 14 additional inelastic pp collisions in the same bunch crossing (known as pile-up).

Monte Carlo simulated event samples are used to optimise the analysis, to compare to the data, and to evaluate signal and background efficiencies and uncertainties. The samples used in the analysis are summarised in Table 1. The main $t\bar{t}$ signal and background samples were processed through the ATLAS detector simulation [21] based on GEANT4 [22]. Some of the systematic uncertainties were studied using alternative $t\bar{t}$ samples processed through a faster simulation making use of parameterised showers in the calorimeters [23]. Additional simulated pp collisions generated with PYTHIA8.186 [24] were overlaid to model the effects from additional collisions in the same and nearby bunch crossings. All simulated events were processed using the same reconstruction algorithms and analysis chain as the data, and small corrections were applied to lepton trigger and reconstruction efficiencies and resolutions to improve the agreement with the response observed in data.

The baseline $t\bar{t}$ simulation sample was produced at next-to-leading order (NLO) in QCD using the matrix-element generator POWHEG-Box v2 [25–27] with CT10 PDFs [10], interfaced to PYTHIA6 [28] with the Perugia 2012 set of tuned parameters (tune) [29] for parton shower, fragmentation and underlying event modelling. The h_{damp} parameter, which gives a cutoff scale for the first gluon emission, was set to m_t , a value which was chosen to give good modelling of the $t\bar{t}$ system p_T at $\sqrt{s} = 7$ TeV [30]. The EVTGEN [31] package was used to better simulate the decay of heavy-flavour hadrons.

Alternative $t\bar{t}$ simulation samples were generated using POWHEG interfaced to HERWIG++ [32], and MADGRAPH5_AMC@NLO [33] interfaced to HERWIG++. The effects of initial- and final-state radiation were explored using two alternative POWHEG + PYTHIA6 samples: one with h_{damp} set to $2m_t$, the factorisation and renormalisation scale varied by a factor of 0.5 and using the Perugia 2012 radHi tune, giving more parton shower radiation; and a second one with the Perugia 2012 radLo tune, $h_{\text{damp}} = m_t$ and the factorisation and renormalisation scale varied by a factor of 2, giving less parton shower radiation. The samples were simulated

following the recommendations documented in Ref. [34]. The top quark mass was set to 172.5 GeV in all these simulation samples and the $t \rightarrow Wb$ branching fraction to 100%.

Backgrounds in this measurement are classified into two types: those with two real prompt leptons from W or Z decays (including those produced via leptonic decays of τ -leptons), and those where at least one of the reconstructed lepton candidates is ‘fake’, i.e. a non-prompt lepton produced from the decay of a bottom or charm hadron, an electron arising from a photon conversion, a jet misidentified as an electron, or a muon produced from an in-flight decay of a pion or kaon. Backgrounds containing two real prompt leptons include single-top production in association with a W boson (Wt), Z + jets production with $Z \rightarrow \tau\tau \rightarrow e\mu$, and diboson production (WW , WZ and ZZ) where both bosons decay leptonically.

The dominant Wt single-top background was modelled using POWHEG-Box v1 + PYTHIA6 with the CT10 PDFs and the Perugia 2012 tune, using the ‘diagram removal’ generation scheme [35]. The Z + jets background was modelled using SHERPA 2.1.1 [36]: matrix elements (ME) were calculated for up to two partons at NLO and four partons at leading order using the COMIX [37] and OPENLOOPS [38] matrix-element generators and merged with the SHERPA parton shower (PS) using the ME + PS@NLO [39] prescription; the CT10 PDF set was used in conjunction with dedicated parton shower tuning in SHERPA. Diboson production with additional jets was also simulated using SHERPA 2.1.1 and CT10 PDFs as described above; the four-lepton final state, the three-lepton final state with two different-flavour leptons, and the two-lepton final state were simulated to cover ZZ , ZW and WW production, and include off-shell Z/γ^* contributions. Same-charge WW production from QCD and electroweak processes was included. Alternative Wt and diboson simulation samples were generated using POWHEG + HERWIG++ and POWHEG + PYTHIA8, respectively, to estimate the background modelling uncertainties.

The majority of the background with at least one fake lepton in the selected sample arises from $t\bar{t}$ production where only one of the W bosons from the top quarks decays leptonically, which was simulated as discussed earlier. Other processes with one real lepton which can contribute to this background include the t -channel single-top production, modelled using POWHEG-Box v1 + PYTHIA6, and W + jets with the W decaying to $e\nu$, $\mu\nu$ or $\tau\nu$ where the τ -lepton subsequently decays leptonically. This background was modelled using POWHEG-Box v2 + PYTHIA8 with the CT10 PDFs. The small expected contribution from $t\bar{t}$ in association with a W or Z boson to the same-charge $e\mu$ sample used for background estimation was modelled using MADGRAPH + PYTHIA8 [40]. Other backgrounds, including processes with two misidentified leptons, are negligible.

3. Object and event selection

This measurement makes use of reconstructed electrons, muons and b -tagged jets. The object and event selections largely follow those used in the earlier publication; in particular the same kinematic cuts are used for electrons and jets, and very similar ones are used for muons.

Electron candidates are reconstructed from an isolated electromagnetic calorimeter energy deposit matched to a track in the inner detector and passing a medium likelihood-based requirement [41,42], within the fiducial region of transverse energy $E_T > 25$ GeV and pseudorapidity¹ $|\eta| < 2.47$. Candidates within the transition region between the barrel and endcap electromagnetic calorimeters, $1.37 < |\eta| < 1.52$, are removed. The electron candidates must satisfy requirements on the transverse impact parameter significance calculated with respect to the beamline of $|d_0|/\sigma_{d_0} < 5$ and on the longitudinal impact parameter calculated with respect to the primary vertex of $|\Delta z_0 \sin \theta| < 0.5$ mm. The primary vertex is defined as the one with the highest sum of p_T^2 of tracks associated to it. Electrons are required to be isolated using requirements on the calorimeter energy in a cone of size $\Delta R < 0.2$ around the electron (excluding the deposit from the electron itself) divided by the electron p_T , and on the sum of track p_T in a variable-size cone around the electron direction (again excluding the electron track itself). The track isolation cone size is given by the smaller of $\Delta R = 10 \text{ GeV}/p_T(e)$ and $\Delta R = 0.2$, i.e. a cone which increases in size at low p_T up to a maximum of 0.2. Selection criteria, dependent on p_T and η , are applied to produce a nominal efficiency of 95% for electrons from $Z \rightarrow ee$ decays with p_T of 25 GeV which rises to 99% at 60 GeV. The efficiencies in $t\bar{t}$ events are smaller, due to the increased jet activity. To prevent double-counting of electron energy deposits as jets, the closest jet with $\Delta R < 0.2$ of a reconstructed electron is removed. Finally, if the nearest jet surviving the above selection is within $\Delta R = 0.4$ of the electron, the electron is discarded, to ensure it is sufficiently separated from nearby jet activity.

Muon candidates are reconstructed by combining matching tracks reconstructed in both the inner detector and muon spectrometer, and are required to satisfy $p_T > 25$ GeV and $|\eta| < 2.4$ [43]. Muons are also required to be isolated, using requirements similar to those for electrons, with the selection criteria tuned to give similar efficiencies for $Z \rightarrow \mu\mu$ events. The muon candidates must satisfy the requirements on the transverse impact parameter significance and on the longitudinal impact parameter of $|d_0|/\sigma_{d_0} < 3$ and $|\Delta z_0 \sin \theta| < 0.5$ mm, respectively. To reduce the background from muons from heavy-flavour decays inside jets, muons are removed if they are separated from the nearest jet by $\Delta R < 0.4$. However, if this jet has fewer than three associated tracks, the muon is kept and the jet is removed instead; this avoids an inefficiency for high-energy muons undergoing significant energy loss in the calorimeter.

Jets are reconstructed using the anti- k_t algorithm [44,45] with radius parameter $R = 0.4$, starting from topological clusters of deposited energy in the calorimeters. Jets are calibrated using an energy- and η -dependent simulation-based calibration scheme with corrections derived from data. No corrections for semileptonic b -hadron decays are applied. Jets are accepted within the fiducial

region $p_T > 25$ GeV and $|\eta| < 2.5$. To reduce the contribution from jets associated with pile-up, jets with $p_T < 50$ GeV and $|\eta| < 2.4$ are required to pass a pile-up rejection veto [46].

Jets are b -tagged as likely to contain b -hadrons using the MV2c20 algorithm [47], a multivariate discriminant making use of track impact parameters and reconstructed secondary vertices and tuned with the new detector configuration, i.e. including the Insertable B-Layer detector (IBL) [20]. Jets are defined as being b -tagged if the MV2c20 weight is larger than a threshold value corresponding to approximately 70% b -tagging efficiency for b -jets in $t\bar{t}$ events, although the exact efficiency varies with p_T . In simulation, the tagging algorithm gives a rejection factor of about 440 against light-quark and gluon jets, and about 8 against jets originating from charm quarks. The improvements of a factor of three in the light-quark rejection and of 60% in the charm-quark rejection compared to the b -tagging algorithm used in Ref. [13] originate from the gain in track impact parameter resolution from the IBL, and improvements in the track reconstruction and b -tagging algorithms [47].

Events are rejected if the selected electron and muon are separated by $\Delta\phi < 0.15$ rad and $\Delta\theta < 0.15$ rad, where $\Delta\phi$ and $\Delta\theta$ are the differences in polar and azimuthal angles between the two leptons. This requirement rejects events where a muon undergoes significant energy loss in the electromagnetic calorimeter, thus leading to a reconstructed electron candidate. Events passing the above requirements, and having exactly one selected electron and one selected muon of opposite electric charge sign (OS), define the $e\mu$ preselected sample. The corresponding same-sign (SS) sample is used in the estimation of background from events with misidentified leptons. Events are then further classified into those with exactly one or exactly two b -tagged jets.

4. Extraction of the $t\bar{t}$ cross-section

The $t\bar{t}$ cross-section is measured in the dileptonic $e\mu$ channel, where one top quark decays as $t \rightarrow Wb \rightarrow e\nu b$ and the other as $t \rightarrow Wb \rightarrow \mu\nu b$.² The final states from leptonic τ decays are also included. As in Ref. [13], $\sigma_{t\bar{t}}$ is determined by counting the numbers of opposite-sign $e\mu$ events with exactly one (N_1) and exactly two (N_2) b -tagged jets, ignoring any jets that are not b -tagged which may be present, due to e.g. light-quark or gluon jets from QCD radiation or b -jets from top quark decays which are not b -tagged. The two event counts can be expressed as:

$$\begin{aligned} N_1 &= L\sigma_{t\bar{t}} \epsilon_{e\mu} 2\epsilon_b(1 - C_b\epsilon_b) + N_1^{\text{bkg}} \\ N_2 &= L\sigma_{t\bar{t}} \epsilon_{e\mu} C_b\epsilon_b^2 + N_2^{\text{bkg}} \end{aligned} \quad (1)$$

where L is the integrated luminosity of the sample and $\epsilon_{e\mu}$ the efficiency for a $t\bar{t}$ event to pass the opposite-sign $e\mu$ preselection. The combined probability for a jet from the quark q in the $t \rightarrow Wq$ decay to fall within the acceptance of the detector, be reconstructed as a jet with transverse momentum above the selection threshold, and be tagged as a b -jet, is denoted by ϵ_b . If the decays of the two top quarks and the subsequent reconstruction of the two b -tagged jets are completely independent, the probability to tag both b -jets ϵ_{bb} is given by $\epsilon_{bb} = \epsilon_b^2$. In practice, small correlations are present for kinematic and instrumental reasons, and these are taken into account via the tagging correlation coefficient C_b , defined as $C_b = \epsilon_{bb}/\epsilon_b^2$ or equivalently $C_b = 4N_{e\mu}^{t\bar{t}} N_2^{t\bar{t}} / (N_1^{t\bar{t}} + 2N_2^{t\bar{t}})^2$, where $N_{e\mu}^{t\bar{t}}$ is the number of preselected $e\mu$ $t\bar{t}$ events and $N_1^{t\bar{t}}$ and $N_2^{t\bar{t}}$ are the numbers of events

¹ ATLAS uses a right-handed coordinate system with its origin at the nominal interaction point (IP) in the centre of the detector and the z -axis along the beam pipe. The x -axis points from the IP to the centre of the LHC ring, and the y -axis points upwards. Cylindrical coordinates (r, ϕ) are used in the transverse plane, ϕ being the azimuthal angle around the z -axis. The pseudorapidity is defined in terms of the polar angle θ as $\eta = -\ln \tan(\theta/2)$. Angular distance is measured in units of $\Delta R \equiv \sqrt{(\Delta\eta)^2 + (\Delta\phi)^2}$.

² This notation indicates the leptonic decay of both t and \bar{t} . Charge-conjugate modes are implied unless otherwise stated.

Table 2

Observed numbers of opposite-sign $e\mu$ events with one and two b -tagged jets (N_1 and N_2), together with the estimates of non- $t\bar{t}$ backgrounds and associated systematic uncertainties. Uncertainties quoted as 0 are < 0.5 .

Event counts	N_1	N_2
Data	11958	7069
Single top	1140 ± 100	221 ± 68
Diboson	34 ± 11	1 ± 0
$Z(\rightarrow \tau\tau \rightarrow e\mu) + \text{jets}$	37 ± 18	2 ± 1
Misidentified leptons	164 ± 65	116 ± 55
Total background	1370 ± 120	340 ± 88

with one and two b -tagged jets. Background from sources other than $t\bar{t} \rightarrow e\mu\nu\bar{\nu}bb$ also contributes to the event counts N_1 and N_2 , and is given by the background terms N_1^{bkg} and N_2^{bkg} . The preselection efficiency $\epsilon_{e\mu}$ and tagging correlation C_b are taken from $t\bar{t}$ event simulation and are about 0.83% and 1.002, respectively, and the background contributions N_1^{bkg} and N_2^{bkg} are estimated using a combination of simulation and data-based methods as described in Section 5, allowing the two equations (1) to be solved yielding $\sigma_{t\bar{t}}$ and ϵ_b by minimising a likelihood function.

In the method to measure the $t\bar{t}$ cross-section outlined above, some of the largest systematic uncertainties come from the use of simulation to estimate the preselection efficiency $\epsilon_{e\mu}$. This efficiency can be factorised into the product of two terms: $\epsilon_{e\mu} = A_{e\mu} G_{e\mu}$. The acceptance $A_{e\mu}$ represents the fraction of $t\bar{t}$ events that have a true $e\mu$ pair within the detector acceptance ($p_T > 25$ GeV and $|\eta| < 2.5$) and it is about 2.7% (2.3% excluding τ decays). The term $G_{e\mu}$ represents the ratio of reconstructed $t\bar{t}$ events to $t\bar{t}$ events with a true $e\mu$ pair within the fiducial region, where the numerator includes the approximately 2% of reconstructed $t\bar{t}$ events where one or both leptons have true $p_T < 25$ GeV. The fiducial cross-section $\sigma_{t\bar{t}}^{\text{fid}}$ is defined as $\sigma_{t\bar{t}}^{\text{fid}} = A_{e\mu} \sigma_{t\bar{t}}$, avoiding the systematic uncertainties associated with the extrapolation from the measured lepton phase space to the full phase space, and measured following the same technique as in Ref. [13]. The contribution of $t\bar{t}$ events produced in the fiducial region with at least one lepton originating via $W \rightarrow \tau \rightarrow l$ decay is estimated from simulation to be $12.2 \pm 0.1\%$.

A total of 30879 data events passed the $e\mu$ opposite-sign preselection. Table 2 shows the number of events with one and two b -tagged jets, together with the estimates of non- $t\bar{t}$ background and their systematic uncertainties discussed below. The ratio of b -tagged events to preselected events (before b -tagging) is higher for 13 TeV than at 7 and 8 TeV due to the larger increase of the $t\bar{t}$ cross-section with \sqrt{s} compared with the $Z + \text{jets}$ and diboson background cross-sections. In simulation, the sample with one b -tagged jet is expected to be about 89% pure in $t\bar{t}$ events, with the dominant background originating from Wt single-top production, and smaller contributions from events with misidentified leptons, $Z + \text{jets}$ and dibosons. The sample with two b -tagged jets is expected to be about 96% pure in $t\bar{t}$ events, with Wt production again being the dominant background.

The distribution of the number of b -tagged jets in opposite-sign $e\mu$ events is shown in Fig. 1, and compared to the baseline and alternative $t\bar{t}$ and background simulation samples. The $t\bar{t}$ contribution is normalised to the theoretical $t\bar{t}$ cross-section prediction at $\sqrt{s} = 13$ TeV of 832 pb. The agreement between data and simulation in the one and two b -tagged bins used for the cross-section measurement is good. However, the data has about 40% more events with three or more b -tags than the baseline simulation, indicating a mismodelling of events with $t\bar{t}$ produced in association with additional heavy-flavour jets, as discussed further

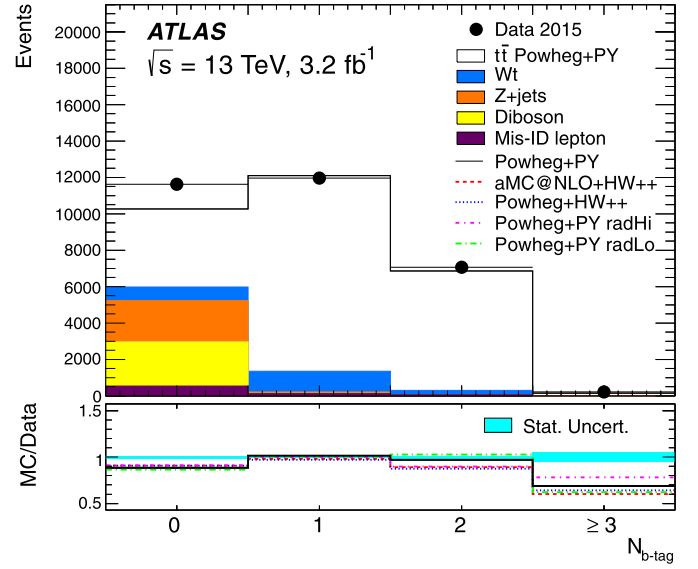


Fig. 1. Distribution of the number of b -tagged jets in preselected opposite-sign $e\mu$ events. The data are shown compared to the prediction from simulation, broken down into contributions from $t\bar{t}$ (using the baseline POWHEG + PYTHIA6 sample), Wt single top, $Z + \text{jets}$, dibosons, and events with fake electrons or muons, normalised to the same integrated luminosity as the data. The lower part of the figure shows the ratio of simulation to data, using various $t\bar{t}$ signal samples, and the shaded band indicates the statistical uncertainty. The $t\bar{t}$ contribution is normalised to the theoretical $t\bar{t}$ cross-section prediction at $\sqrt{s} = 13$ TeV of 832 pb.

in Section 6. There is also an approximately 11% excess of data over simulation for events with zero b -tagged jets which does not affect the measurement, and is compatible with the expected uncertainties in modelling WW [48] and $Z + \text{jets}$ production. Distributions of the number of jets, the jet p_T , and the electron and muon $|\eta|$ and p_T are shown for opposite-sign $e\mu$ events with at least one b -tagged jet in Fig. 2, where the simulation is normalised to the same number of events as the data. In general, the data and simulation agree well.

5. Background estimation

Most background contributions are estimated from simulation. The Wt single-top background is normalised to the approximate NNLO cross-section of 71.7 ± 3.8 pb, determined as in Ref. [49]. The diboson background normalisation is estimated using SHERPA as discussed in Section 2. The normalisation of the $Z + \text{jets}$ background, originating from events with a $Z \rightarrow \tau\tau \rightarrow e\mu$ decay accompanied by one or two b -tagged jets, is determined by scaling the SHERPA simulation with scale factors obtained in $Z \rightarrow ee$ and $Z \rightarrow \mu\mu$ events as described in Section 6.

The background from events with one real and one misidentified lepton is estimated from a combination of data and simulation, using the method employed in Ref. [13]. Simulation studies show that the samples with a same-sign $e\mu$ pair and one or two b -tagged jets are dominated by events with a misidentified lepton, with rates comparable to those in the opposite-sign sample. The contributions of events with misidentified leptons are therefore estimated using the same-sign event counts in data after subtraction of the estimated prompt same-sign contributions, multiplied by the opposite- to same-sign fake-lepton ratios R_j for $j = 1$ and 2 b -tagged jets predicted from simulation. The results are shown in Table 2 and the procedure is illustrated in Table 3, which shows the expected breakdown of same-sign event counts in terms of prompt-lepton and misidentified-lepton events, and the corresponding predictions for misidentified leptons in the

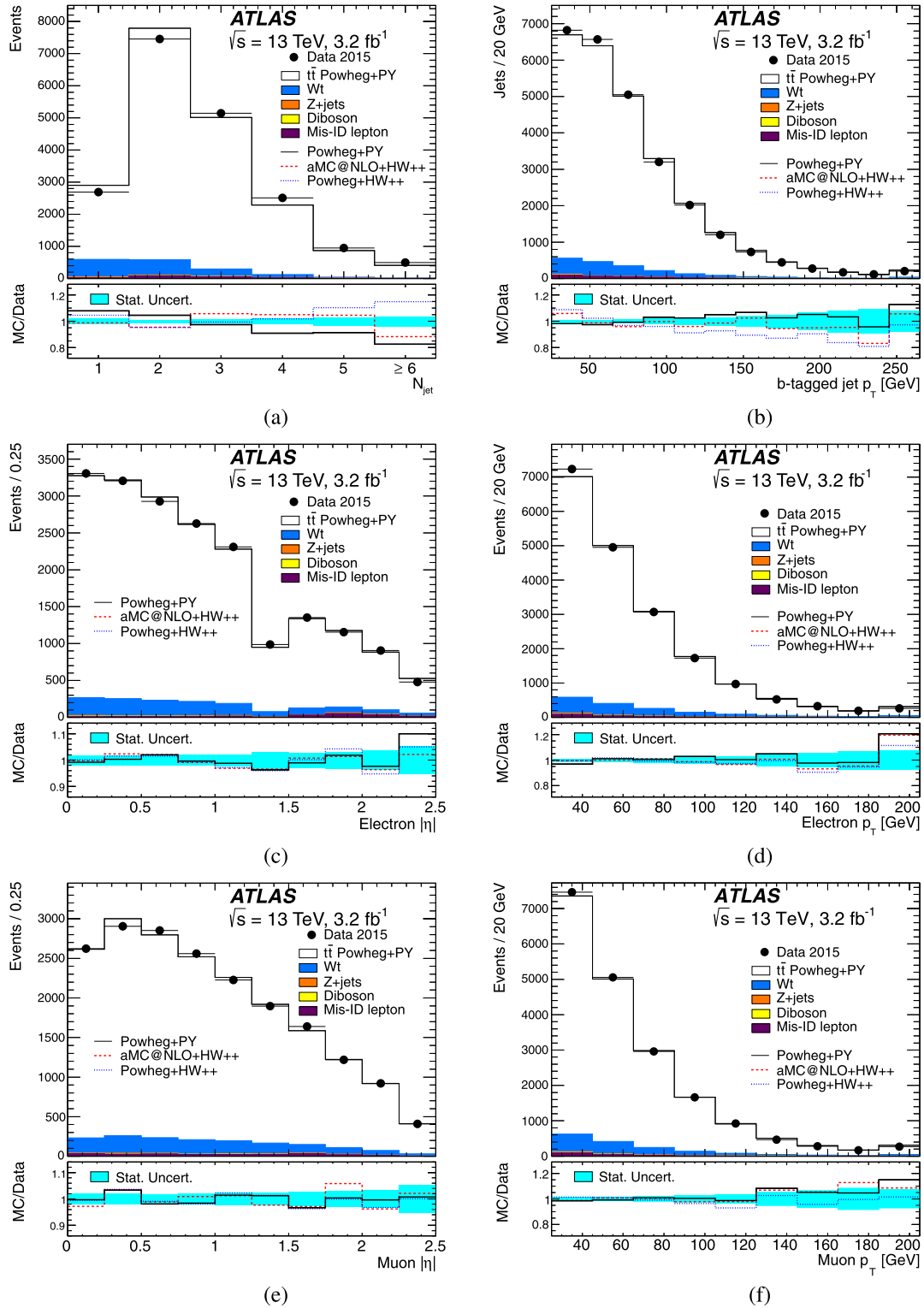


Fig. 2. Distributions of (a) the number of jets, (b) the transverse momentum p_T of the b -tagged jets, (c) the $|\eta|$ of the electron, (d) the p_T of the electron, (e) the $|\eta|$ of the muon and (f) the p_T of the muon, in events with an opposite-sign $e\mu$ pair and at least one b -tagged jet. The data are compared to the prediction from simulation, broken down into contributions from $t\bar{t}$ (using the baseline PowHEG + PYTHIA6 sample), single top, Z + jets, dibosons, and events with fake electrons or muons, normalised to the same number of entries as the data. The lower parts of the figures show the ratios of simulation to data, using various $t\bar{t}$ signal samples, and with the shaded band indicating the statistical uncertainty. The last histogram bin includes the overflow.

opposite-sign sample with all contributions estimated from simulation. The misidentified-lepton contributions are classified into those where the electron is from a photon conversion, from the decay of a heavy-flavour hadron or from other sources (e.g. a

misidentified hadron within a jet), or the muon is from a heavy-flavour decay or other sources (e.g. a pion or kaon decay). The values of R_j are taken to be $R_1 = 1.55 \pm 0.50$ and $R_2 = 1.99 \pm 0.82$, where the central values are taken from ratios of the total numbers

Table 3

The expected numbers of events with at least one misidentified lepton in the one- and two- b -tag opposite- and same-sign $e\mu$ samples, broken down into different categories as described in the text. For the same-sign samples, the contributions from wrong-sign (where the electron charge sign is misreconstructed) and right-sign prompt lepton events are also shown, and the total expected numbers of events are compared to the data. The uncertainties are due to simulation statistics, and numbers quoted as '0.0' are smaller than 0.05.

Component	OS 1b	SS 1b	OS 2b	SS 2b
Conversion e	113 ± 5	83 ± 5	60 ± 3	33.3 ± 1.7
Heavy-flavour e	11.0 ± 1.8	9.8 ± 0.9	1.1 ± 0.3	0.9 ± 0.3
Other e	15 ± 13	0.4 ± 0.2	3.3 ± 1.9	0.2 ± 0.1
Heavy-flavour μ	9.5 ± 0.9	5.6 ± 0.7	1.9 ± 0.4	0.5 ± 0.2
Other μ	3.4 ± 0.5	0.3 ± 0.2	2.7 ± 0.5	0.0 ± 0.0
Total misidentified	151 ± 14	99 ± 5	69 ± 4	35 ± 2
Wrong-sign prompt	–	30.0 ± 1.6	–	16.0 ± 1.1
Right-sign prompt	–	11.8 ± 0.5	–	4.4 ± 0.2
Total	–	141 ± 6	–	55 ± 2
Data	–	149	–	79

of misidentified-lepton events in opposite- and same-sign samples. The uncertainties encompass the different values of R_j predicted for the various sub-components of the misidentified-lepton

background separately, allowing the background composition to be significantly different from that predicted by simulation, where it is dominated by electrons from photon conversions, followed by electrons and muons from the decays of heavy-flavour hadrons. A 50% uncertainty is assigned to the prompt same-sign contribution, which includes events where the charge of the electron was misidentified (denoted by wrong-sign prompt in Table 3) or right-sign with two genuine same-sign leptons (e.g. from $t\bar{t}W/Z$ production). The largest uncertainties in the misidentified-lepton background come from the uncertainties in R_j .

The modelling in simulation of the different components of the misidentified-lepton background is checked by studying kinematic distributions of same-sign events, as illustrated for the p_T and $|\eta|$ distributions of the leptons in events with at least one b -tagged jet in Fig. 3. The simulation models the shapes of the distributions well, but underestimates the number of data events with two b -tagged jets by about 40%, as shown in Table 3. This deficit in simulation is attributed to a larger rate of misidentified-lepton events in data, which increases the estimate of misidentified leptons in the opposite-sign two- b -tag sample accordingly. The modelling is also checked in same-sign control samples with relaxed isolation cuts, enhancing the contributions of heavy-flavour decays, and similar levels of agreement were found, giving confidence that

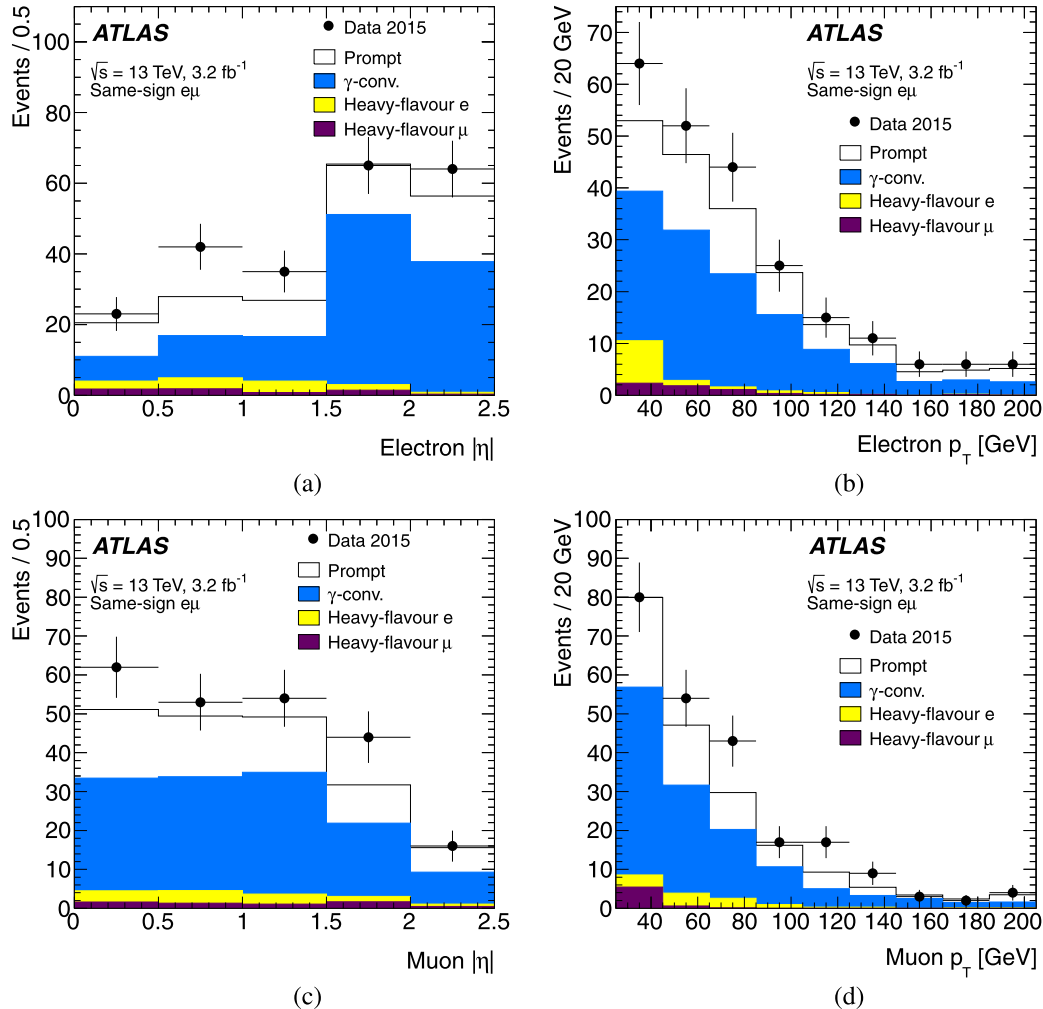


Fig. 3. Distributions of electron and muon $|\eta|$ and p_T in same-sign $e\mu$ events with at least one b -tagged jet. The simulation prediction is normalised to the same integrated luminosity as the data, and broken down into contributions where both leptons are prompt, or one is a misidentified lepton from a photon conversion or heavy-flavour decay. In the p_T distributions, the last bin includes the overflow.

Table 4

Summary of the systematic uncertainties in $\epsilon_{e\mu}$, $G_{e\mu}$ and C_b (with their relative signs where relevant), and the statistical, systematic, luminosity and beam energy uncertainties in the measured $t\bar{t}$ cross-section $\sigma_{t\bar{t}}$ at $\sqrt{s} = 13$ TeV. All uncertainties from the inclusive cross-section measurement apply to the fiducial measurement; in the lower part of the table only the systematic uncertainties that are different for the measurement of the fiducial cross-section $\sigma_{t\bar{t}}^{\text{fid}}$ are given, together with the total analysis systematic uncertainties and total uncertainties in $\sigma_{t\bar{t}}^{\text{fid}}$. Uncertainties quoted as '0.0' are smaller than 0.05%, whilst '-' indicates that the corresponding uncertainty is not applicable.

Uncertainty (inclusive $\sigma_{t\bar{t}}$)	$\Delta\epsilon_{e\mu}/\epsilon_{e\mu}$ [%]	$\Delta C_b/C_b$ [%]	$\Delta\sigma_{t\bar{t}}/\sigma_{t\bar{t}}$ [%]
Data statistics			0.9
$t\bar{t}$ NLO modelling	0.7	−0.1	0.8
$t\bar{t}$ hadronisation	−2.4	0.4	2.8
Initial- and final-state radiation	−0.3	0.1	0.4
$t\bar{t}$ heavy-flavour production	−	0.4	0.4
Parton distribution functions	0.5	−	0.5
Single-top modelling	−	−	0.3
Single-top/ $t\bar{t}$ interference	−	−	0.6
Single-top Wt cross-section	−	−	0.5
Diboson modelling	−	−	0.1
Diboson cross-sections	−	−	0.0
$Z + \text{jets}$ extrapolation	−	−	0.2
Electron energy scale/resolution	0.2	0.0	0.2
Electron identification	0.3	0.0	0.3
Electron isolation	0.4	−	0.4
Muon momentum scale/resolution	−0.0	0.0	0.0
Muon identification	0.4	0.0	0.4
Muon isolation	0.2	−	0.3
Lepton trigger	0.1	0.0	0.2
Jet energy scale	0.3	0.1	0.3
Jet energy resolution	−0.1	0.0	0.2
b -tagging	−	0.1	0.3
Misidentified leptons	−	−	0.6
Analysis systematics	2.7	0.6	3.3
Integrated luminosity	−	−	2.3
LHC beam energy	−	−	1.5
Total uncertainty	2.7	0.6	4.4

Uncertainty (fiducial $\sigma_{t\bar{t}}^{\text{fid}}$)	$\Delta G_{e\mu}/G_{e\mu}$ [%]	$\Delta C_b/C_b$ [%]	$\Delta\sigma_{t\bar{t}}^{\text{fid}}/\sigma_{t\bar{t}}^{\text{fid}}$ [%]
$t\bar{t}$ NLO modelling	0.5	−0.1	0.6
$t\bar{t}$ hadronisation	−1.6	0.4	1.9
Parton distribution functions	0.1	−	0.1
Other uncertainties (as above)	0.8	0.4	1.5
Analysis systematics ($\sigma_{t\bar{t}}^{\text{fid}}$)	1.8	0.6	2.5
Total uncertainty ($\sigma_{t\bar{t}}^{\text{fid}}$)	1.8	0.6	3.9

the simulation adequately models the different sources of misidentified leptons in the selected sample.

6. Systematic uncertainties

The systematic uncertainties in the extracted cross-sections, $\sigma_{t\bar{t}}$ and $\sigma_{t\bar{t}}^{\text{fid}}$, are shown in Table 4, together with their effects (where relevant) on the $t\bar{t}$ preselection efficiency $\epsilon_{e\mu}$, tagging correlation C_b and reconstruction efficiency $G_{e\mu}$. Each source of uncertainty is evaluated by repeating the cross-section extraction with all relevant input parameters simultaneously changed by ± 1 standard deviation. Correlations between input parameters (in particular significant anti-correlations between $\epsilon_{e\mu}$ and C_b which contribute with opposite signs to $\sigma_{t\bar{t}}$) are thus taken into account. The total uncertainties are calculated by adding the effects of all the individual systematic components in quadrature, assuming them to be independent. The sources of systematic uncertainty are discussed in detail below.

$t\bar{t}$ modelling: The modelling uncertainties in $\epsilon_{e\mu}$ and C_b due to the choice of $t\bar{t}$ generator are assessed by comparing the predictions of the baseline POWHEG + PYTHIA6 sam-

ple with the various alternative samples discussed in Section 2. Three separate uncertainties are considered: the NLO generator uncertainty (evaluated by considering the relative difference between MADGRAPH5_AMC@NLO + HERWIG++ and POWHEG + HERWIG++), the parton shower and hadronisation uncertainty (evaluated by considering the relative difference between POWHEG + PYTHIA6 and POWHEG + HERWIG++), and the radiation uncertainty (evaluated by considering half the relative difference between the POWHEG + PYTHIA6 samples with more or less radiation). The prediction for $\epsilon_{e\mu}$ is found to be particularly sensitive to the amount of hadronic activity near the leptons, which strongly affects the efficiency of the lepton isolation requirements described in Section 3. These isolation efficiencies are therefore measured directly from data, as discussed below, and thus no modelling uncertainty is considered for the lepton isolation. Motivated by the level of agreement for events with at least three b -tags seen in Fig. 1, an additional uncertainty in C_b is determined by calculating in data and simulation the ratio R_{32} of the number of events with at least three

b -tagged jets to the number with at least two. The baseline simulation sample is reweighted to change the fraction of events with at least three b -jets at generator level, which effectively changes the $t\bar{t}$ plus heavy-flavour fraction and the values of both C_b and R_{32} . A linear relation between changes in C_b and R_{32} is found, and used to translate the difference between the R_{32} values found in data ($3.1 \pm 0.2\%$) and simulation ($2.21 \pm 0.05\%$) to a shift in C_b of 0.39%. This shift is treated as an additional uncertainty in C_b due to the modelling of heavy-flavour production in $t\bar{t}$ events, uncorrelated to the NLO, hadronisation and radiation uncertainties discussed above.

Parton distribution functions: The uncertainties in $\epsilon_{e\mu}$ and C_b due to limited knowledge of the proton PDFs are evaluated by reweighting simulated events produced with MADGRAPH5_AMC@NLO using the error sets of the NNPDF 3.0 PDF sets [50]. The eigenvectors consist of a central PDF and 100 Monte Carlo replicas, for which the root mean square was taken to calculate the uncertainty. The MADGRAPH5_AMC@NLO sample was produced with CT10; therefore the cross-section was corrected for the relative difference between the central prediction of CT10 and NNPDF 3.0, which is about 1%. The uncertainty using the PDF4LHC Run-2 recommendations with 100 eigenvectors [51] is very similar to that obtained with NNPDF 3.0.

Single-top modelling: The uncertainties related to Wt single-top modelling are assessed by comparing the predictions of POWHEG + PYTHIA6 and POWHEG + HERWIG++ and considering the relative difference, comparing the diagram removal and diagram subtraction schemes for dealing with the interference between the $t\bar{t}$ and Wt final states, and also considering half the relative difference between the POWHEG + PYTHIA6 samples with more or less radiation. Production of single top quarks via the t - and s -channels gives rise to final states with only one prompt lepton, and is accounted for as part of the misidentified-lepton background.

Diboson modelling: The uncertainties in the background contributions from dibosons with one or two additional b -tagged jets were assessed by comparing the baseline prediction from SHERPA with that of POWHEG + PYTHIA8. These uncertainties have a limited effect on the cross-section measurement due to the small number of diboson background events.

Background cross-sections: The uncertainties in the Wt single-top and diboson cross-sections are taken to be 5.3% [49] and 6% [52], based on the corresponding theoretical predictions.

Z + jets extrapolation: The cross-sections for Z + jets and especially Z + heavy-flavour jets are subject to large theoretical uncertainties, making purely simulation-based estimates unreliable. This background was therefore determined by measuring the rates of $Z \rightarrow ee$ and $Z \rightarrow \mu\mu$ events with one and two b -tagged jets in both data and simulation, and using the resulting ratio to scale the simulation estimate of background from $Z \rightarrow \tau\tau$ + jets. The Z + jets background prediction from simulation was scaled by 1.1 for the background with one b -tagged jet and by 1.2 for the background with two b -tagged jets. A 50% uncertainty was applied to the Z + jets contributions which cover the differences observed on the event yields comparing Z + jets SHERPA vs POWHEG + PYTHIA8.

Lepton-related uncertainties: The modelling of the electron and muon trigger efficiencies, identification efficiencies, energy scales and resolutions are studied using $Z \rightarrow ee$ and

$Z \rightarrow \mu\mu$ decays in data and simulation. Small corrections are applied to the simulation to improve the agreement with the response observed in data. These corrections have associated uncertainties that are propagated to the cross-section measurement. The uncertainty in the trigger efficiency is small compared to those for electron or muon identification since most events are triggered redundantly by both leptons. The efficiency of the lepton isolation requirements was measured directly in data $t\bar{t}$ events, thus including the effects of pile-up, by relaxing the cuts alternately on electrons and muons as in Ref. [13]. The results, after the correction for the contamination from misidentified leptons estimated using the same-sign $e\mu$ samples as described in Section 5, showed that the baseline POWHEG + PYTHIA6 simulation overestimates the efficiencies of the isolation requirements by about 0.2% for both the electrons and muons. These corrections were applied to $\epsilon_{e\mu}$ and the corresponding uncertainties are dominated by the subtraction of misidentified leptons.

Jet-related uncertainties: Although the efficiency to reconstruct and b -tag jets from $t\bar{t}$ events is extracted from the data, uncertainties in the jet energy scale, energy resolution and reconstruction efficiency affect the backgrounds estimated from simulation and the estimate of the tagging correlation C_b . They also have a small effect on $\epsilon_{e\mu}$ via the lepton-jet ΔR separation cuts. The jet energy scale is varied in simulation according to the uncertainties derived from the $\sqrt{s} = 8$ TeV simulation and data calibration, extrapolated to $\sqrt{s} = 13$ TeV [53]. The uncertainties are evaluated using a model with 19 separate orthogonal components and the resulting variations were added in quadrature. The jet energy resolution uncertainty is also assessed using $\sqrt{s} = 8$ TeV data, and extrapolated to $\sqrt{s} = 13$ TeV.

b -tagging uncertainties: The correlation factor C_b depends weakly on the b -tagging and mistagging efficiencies predicted by the simulation, as it is evaluated from the numbers of events with one and two b -tagged jets. The uncertainties are determined from $\sqrt{s} = 8$ TeV data, with additional uncertainties to account for the presence of the newly-installed insertable B-layer detector (IBL) [20] and the extrapolation to $\sqrt{s} = 13$ TeV. Since the definition of $\epsilon_{e\mu}$ does not involve b -tagged jets, it has no b -tagging or mistagging-related uncertainties.

Misidentified leptons: The uncertainties in the number of events with misidentified leptons in the one and two b -tagged samples are derived from the statistical uncertainties in the numbers of same-sign lepton events, the systematic uncertainties in the opposite- to same-sign ratios R_j , and the uncertainties in the numbers of prompt same-sign events, as discussed in detail in Section 5.

Integrated luminosity: The uncertainty in the integrated luminosity is 2.1%. It is derived, following a methodology similar to that detailed in Ref. [54], from a calibration of the luminosity scale using x - y beam-separation scans performed in August 2015. The effect on the cross-section measurement is slightly larger than 2.1% because the Wt single-top and diboson backgrounds are evaluated from simulation, so they are also sensitive to the assumed integrated luminosity.

LHC beam energy: The LHC beam energy during the 2012 pp run was calibrated to be $0.30 \pm 0.66\%$ smaller than the nominal value of 4 TeV per beam, using the revolution frequency difference of protons and lead ions during p + Pb

runs in early 2013 [55]. This relative uncertainty is also applicable to the 2015 pp run. Since this calibration is compatible with the nominal centre-of-mass energy of 13 TeV, no correction is applied to the measured $\sigma_{t\bar{t}}$ value. However, an uncertainty of 1.5%, corresponding to the expected change in $\sigma_{t\bar{t}}$ for a 0.66% change in centre-of-mass energy, is quoted separately for the final result.

Top quark mass: Alternative $t\bar{t}$ samples generated with different m_t from 170 to 177.5 GeV are used to quantify the dependence of the acceptance for $t\bar{t}$ events on the assumed m_t value. The level of Wt single-top background based on the change of the Wt cross-section for the same mass range is also considered. The $t\bar{t}$ acceptance and background effects partially cancel, and the final dependence of the result on the assumed m_t value is determined to be $d\sigma_{t\bar{t}}/dm_t = -0.3\%/GeV$. The result of the analysis is reported for a top quark mass of 172.5 GeV, and the small dependence of the cross-section on the assumed mass is not included in the total systematic uncertainty.

The total systematic uncertainties in $\epsilon_{e\mu}$, C_b , $G_{e\mu}$ and the fitted values of $\sigma_{t\bar{t}}$ and $\sigma_{t\bar{t}}^{\text{fid}}$ are shown in Table 4, and the total systematic uncertainties in the individual background components are shown in Table 2. The dominant uncertainties in the cross-section result come from the luminosity determination and $t\bar{t}$ modelling, in particular from the $t\bar{t}$ shower and hadronisation uncertainty.

7. Results and conclusions

The inclusive $t\bar{t}$ production cross-section is measured in the dilepton $t\bar{t} \rightarrow e\mu\nu\bar{\nu}b\bar{b}$ decay channel using 3.2 fb^{-1} of $\sqrt{s} = 13 \text{ TeV}$ pp collisions recorded by the ATLAS detector at the LHC. The numbers of opposite-sign $e\mu$ events with one and two b -tagged jets are counted, allowing a simultaneous determination of the $t\bar{t}$ cross-section $\sigma_{t\bar{t}}$ and the probability to reconstruct and b -tag a jet from a $t\bar{t}$ decay. Assuming a top quark mass of $m_t = 172.5 \text{ GeV}$, the result is:

$$\sigma_{t\bar{t}} = 818 \pm 8 \text{ (stat)} \pm 27 \text{ (syst)} \pm 19 \text{ (lumi)} \pm 12 \text{ (beam) pb},$$

where the four uncertainties are due to data statistics, experimental and theoretical systematic effects, the integrated luminosity and the LHC beam energy, giving a total relative uncertainty of 4.4%. The combined probability for a jet from a top quark decay to be within the detector acceptance and tagged as a b -jet is measured to be $\epsilon_b = 0.559 \pm 0.004 \pm 0.003$, where the first error is statistical and the second systematic, in fair agreement with the nominal prediction from simulation of 0.549.

This cross-section measurement is consistent with the theoretical prediction based on NNLO + NNLL calculations of $832^{+40}_{-46} \text{ pb}$ at $m_t = 172.5 \text{ GeV}$. Fig. 4 shows the result of this $\sigma_{t\bar{t}}$ measurement together with the most precise ATLAS results at $\sqrt{s} = 7$ and 8 TeV [13]. The data are compared to the NNLO + NNLL predictions as a function of the centre-of-mass energy. The result is also consistent with a recent measurement by CMS at $\sqrt{s} = 13 \text{ TeV}$ using a smaller data sample [56].

The measured fiducial cross-section $\sigma_{t\bar{t}}^{\text{fid}}$ for a $t\bar{t}$ event producing an $e\mu$ pair, each lepton originating directly from $t \rightarrow W \rightarrow \ell$ or via a leptonic τ decay $t \rightarrow W \rightarrow \tau \rightarrow \ell$ and satisfying $p_T > 25 \text{ GeV}$ and $|\eta| < 2.5$ is:

$$\sigma_{t\bar{t}}^{\text{fid}} = 11.32 \pm 0.10 \text{ (stat)} \pm 0.29 \text{ (syst)} \pm 0.26 \text{ (lumi)} \pm 0.17 \text{ (beam) pb},$$

with uncertainties due to data statistics, systematic effects, the knowledge of the integrated luminosity and the LHC beam energy, corresponding to a total relative uncertainty of 3.9% and an

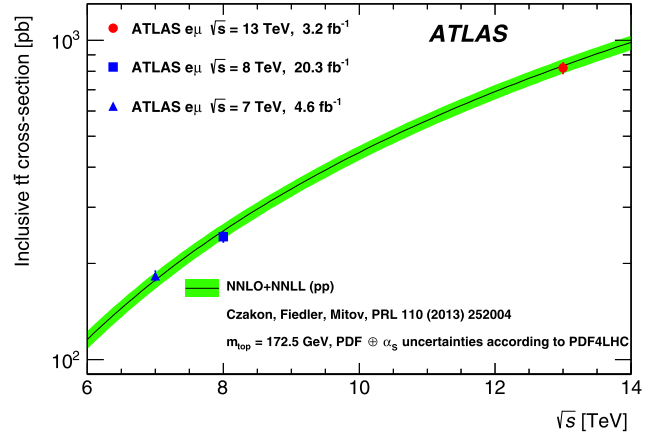


Fig. 4. Cross-section for $t\bar{t}$ pair production in pp collisions as a function of centre-of-mass energy. ATLAS results in the dilepton $e\mu$ channel at $\sqrt{s} = 13, 8$ and 7 TeV are compared to the NNLO + NNLL theoretical predictions.

internal systematic uncertainty excluding the luminosity and the LHC beam energy of 2.5%. The breakdown of the systematic uncertainties is presented in Table 4. Overall, the analysis systematic uncertainties in the fiducial cross-section are smaller than those in the inclusive cross-section, due to the substantial reductions in the PDF and hadronisation uncertainties that contribute significantly to both the acceptance $A_{e\mu}$ and reconstruction efficiency $G_{e\mu}$.

Acknowledgements

We thank CERN for the very successful operation of the LHC, as well as the support staff from our institutions without whom ATLAS could not be operated efficiently.

We acknowledge the support of ANPCyT, Argentina; YerPhI, Armenia; ARC, Australia; BMWFW and FWF, Austria; ANAS, Azerbaijan; SSTC, Belarus; CNPq and FAPESP, Brazil; NSERC, NRC and CFI, Canada; CERN; CONICYT, Chile; CAS, MOST and NSFC, China; COLCIENCIAS, Colombia; MSMT CR, MPO CR and VSC CR, Czech Republic; DNRF and DNSRC, Denmark; IN2P3-CNRS, CEA-DSM/IRFU, France; GNSF, Georgia; BMBF, HGF, and MPG, Germany; GSRT, Greece; RGC, Hong Kong SAR, China; ISF, I-CORE and Benoziyo Center, Israel; INFN, Italy; MEXT and JSPS, Japan; CNRST, Morocco; FOM and NWO, Netherlands; RCN, Norway; MNiSW and NCN, Poland; FCT, Portugal; MNE/IFA, Romania; MES of Russia and NRC KI, Russian Federation; JINR; MESTD, Serbia; MSSR, Slovakia; ARRS and MIZŠ, Slovenia; DST/NRF, South Africa; MINECO, Spain; SRC and Wallenberg Foundation, Sweden; SERI, SNSF and Cantons of Bern and Geneva, Switzerland; MOST, Taiwan; TAEK, Turkey; STFC, United Kingdom; DOE and NSF, United States of America. In addition, individual groups and members have received support from BCKDF, the Canada Council, Canarie, CRC, Compute Canada, FQRNT, and the Ontario Innovation Trust, Canada; EPLANET, ERC, FP7, Horizon 2020 and Marie Skłodowska-Curie Actions, European Union; Investissements d'Avenir Labex and Idex, ANR, Région Auvergne and Fondation Partager le Savoir, France; DFG and AvH Foundation, Germany; Herakleitos, Thales and Aristeia programmes co-financed by EU-ESF and the Greek NSRF; BSF, GIF and Minerva, Israel; BRF, Norway; Generalitat de Catalunya, Generalitat Valenciana, Spain; the Royal Society and Leverhulme Trust, United Kingdom.

The crucial computing support from all WLCG partners is acknowledged gratefully, in particular from CERN, the ATLAS Tier-1 facilities at TRIUMF (Canada), NDGF (Denmark, Norway, Sweden), CC-IN2P3 (France), KIT/GridKA (Germany), INFN-CNAF (Italy), NL-T1 (Netherlands), PIC (Spain), ASGC (Taiwan), RAL (UK) and BNL (USA), the Tier-2 facilities worldwide and large non-WLCG resource

providers. Major contributors of computing resources are listed in Ref. [57].

References

- [1] M. Cacciari, et al., Top-pair production at hadron colliders with next-to-next-to-leading logarithmic soft-gluon resummation, *Phys. Lett. B* 710 (2012) 612, arXiv:1111.5869 [hep-ph].
- [2] P. Bärnreuther, et al., Percent level precision physics at the LHC: first genuine NNLO QCD corrections to $q\bar{q} \rightarrow t\bar{t} + X$, *Phys. Rev. Lett.* 109 (2012) 132001, arXiv:1204.5201 [hep-ph].
- [3] M. Czakon, A. Mitov, NNLO corrections to top-pair production at hadron colliders: the all-fermionic scattering channels, *J. High Energy Phys.* 1212 (2012) 054, arXiv:1207.0236 [hep-ph].
- [4] M. Czakon, A. Mitov, NNLO corrections to top pair production at hadron colliders: the quark-gluon reaction, *J. High Energy Phys.* 1301 (2013) 080, arXiv:1210.6832 [hep-ph].
- [5] M. Czakon, P. Fiedler, A. Mitov, The total top quark pair production cross-section at hadron colliders through $\mathcal{O}(\alpha_s^4)$, *Phys. Rev. Lett.* 110 (2013) 252004, arXiv:1303.6254 [hep-ph].
- [6] M. Czakon, A. Mitov, Top++: a program for the calculation of the top-pair cross-section at hadron colliders, *Comput. Phys. Commun.* 185 (2014) 2930, arXiv:1112.5675 [hep-ph].
- [7] M. Botje, et al., The PDF4LHC Working Group Interim Recommendations, arXiv:1101.0538 [hep-ph], 2011.
- [8] A.D. Martin, et al., Parton distributions for the LHC, *Eur. Phys. J. C* 63 (2009) 189, arXiv:0901.0002 [hep-ph].
- [9] A.D. Martin, et al., Uncertainties on α_s in global PDF analyses and implications for predicted hadronic cross sections, *Eur. Phys. J. C* 64 (2009) 653, arXiv:0905.3531 [hep-ph].
- [10] H.L. Lai, et al., New parton distributions for collider physics, *Phys. Rev. D* 82 (2010) 074024, arXiv:1007.2241 [hep-ph].
- [11] J. Gao, et al., The CT10 NNLO global analysis of QCD, *Phys. Rev. D* 89 (2014) 033009, arXiv:1302.6246 [hep-ph].
- [12] R.D. Ball, et al., Parton distributions with LHC data, *Nucl. Phys. B* 867 (2013) 244–289, arXiv:1207.1303 [hep-ph].
- [13] ATLAS Collaboration, Measurement of the $t\bar{t}$ production cross-section using $e\mu$ events with b -tagged jets in pp collisions at $\sqrt{s} = 7$ and 8 TeV with the ATLAS detector, *Eur. Phys. J. C* 74 (2014) 3109, arXiv:1406.5375 [hep-ex].
- [14] ATLAS Collaboration, Measurement of the top pair production cross section in 8 TeV proton–proton collisions using kinematic information in the lepton + jets final state with ATLAS, *Phys. Rev. D* 91 (2015) 112013, arXiv:1504.04251 [hep-ex].
- [15] ATLAS Collaboration, Measurement of the top quark pair production cross-section with ATLAS in the single lepton channel, *Phys. Lett. B* 711 (2012) 244, arXiv:1201.1889 [hep-ex].
- [16] CMS Collaboration, Measurement of the $t\bar{t}$ production cross section in the $e\mu$ channel in proton–proton collisions at $\sqrt{s} = 7$ and 8 TeV, arXiv:1603.02303 [hep-ex], 2016.
- [17] CMS Collaboration, Measurements of the $t\bar{t}$ production cross section in lepton + jets final states in pp collisions at 8 TeV and ratio of 8 to 7 TeV cross sections, arXiv:1602.09024 [hep-ex], 2016.
- [18] CMS Collaboration, Measurement of the $t\bar{t}$ production cross section in pp collisions at $\sqrt{s} = 7$ TeV with lepton + jets final states, *Phys. Lett. B* 720 (2013) 83–104, arXiv:1212.6682 [hep-ex].
- [19] ATLAS Collaboration, The ATLAS experiment at the CERN Large Hadron Collider, *J. Instrum.* 3 (2008), S08003.
- [20] ATLAS Collaboration, ATLAS Insertable B-Layer Technical Design Report, ATLAS-TDR-19, <http://cdsweb.cern.ch/record/1291633>, 2010.
- [21] ATLAS Collaboration, The ATLAS simulation infrastructure, *Eur. Phys. J. C* 70 (2010) 823, arXiv:1005.4568 [hep-ex].
- [22] S. Agostinelli, et al., GEANT4: a simulation toolkit, *Nucl. Instrum. Methods A* 506 (2003) 250.
- [23] ATLAS Collaboration, The simulation principle and performance of the ATLAS fast calorimeter simulation FastCaloSim, ATLAS-PHYS-PUB-2010-013, <http://cdsweb.cern.ch/record/1300517>, 2010.
- [24] T. Sjöstrand, S. Mrenna, P. Skands, A brief introduction to Pythia 8.1, *Comput. Phys. Commun.* 178 (2008) 852, arXiv:0710.3820 [hep-ph].
- [25] P. Nason, A new method for combining NLO QCD with shower Monte Carlo algorithms, *J. High Energy Phys.* 0411 (2004) 040, arXiv:hep-ph/0409146.
- [26] S. Frixione, P. Nason, C. Oleari, Matching NLO QCD computations with parton shower simulations: the POWHEG method, *J. High Energy Phys.* 0711 (2007) 070, arXiv:0709.2092 [hep-ph].
- [27] S. Alioli, et al., A general framework for implementing NLO calculations in shower Monte Carlo programs: the POWHEG BOX, *J. High Energy Phys.* 1006 (2010) 043, arXiv:1002.2581 [hep-ph].
- [28] T. Sjöstrand, S. Mrenna, P. Skands, Pythia 6.4 physics and manual, *J. High Energy Phys.* 0605 (2006) 026, arXiv:hep-ph/0603175.
- [29] P.Z. Skands, Tuning Monte Carlo generators: the Perugia tunes, *Phys. Rev. D* 82 (2010) 074018, arXiv:1005.3457 [hep-ph].
- [30] ATLAS Collaboration, Comparison of Monte Carlo generator predictions to ATLAS measurements of top pair production at $\sqrt{s} = 7$ TeV, ATLAS-PHYS-PUB-2015-002, <http://cdsweb.cern.ch/record/1981319>, 2015.
- [31] D.J. Lange, The EvtGen particle decay simulation package, *Nucl. Instrum. Methods A* 462 (2001) 152–155.
- [32] M. Bahr, et al., Herwig++ physics and manual, *Eur. Phys. J. C* 58 (2008) 639–707, arXiv:0803.0883 [hep-ph].
- [33] J. Alwall, et al., The automated computation of tree-level and next-to-leading order differential cross sections, and their matching to parton shower simulations, *J. High Energy Phys.* 1407 (2014) 079, arXiv:1405.0301 [hep-ph].
- [34] ATLAS Collaboration, Simulation of top-quark production for the ATLAS experiment at $\sqrt{s} = 13$ TeV, ATLAS-PHYS-PUB-2016-004, <http://cdsweb.cern.ch/record/2120417>, 2016.
- [35] S. Frixione, et al., Single-top hadroproduction in association with a W boson, *J. High Energy Phys.* 0807 (2008) 029, arXiv:0805.3067 [hep-ph].
- [36] T. Gleisberg, et al., Event generation with SHERPA 1.1, *J. High Energy Phys.* 0902 (2009) 007, arXiv:0811.4622 [hep-ph].
- [37] T. Gleisberg, S. Höche, Comix, a new matrix element generator, *J. High Energy Phys.* 0812 (2008) 039, arXiv:0808.3674 [hep-ph].
- [38] F. Cascioli, P. Maierhofer, S. Pozzorini, Scattering amplitudes with open loops, *Phys. Rev. Lett.* 108 (2012) 111601, arXiv:1111.5206 [hep-ph].
- [39] S. Höche, et al., QCD matrix elements + parton showers: the NLO case, *J. High Energy Phys.* 1304 (2013) 027, arXiv:1207.5030 [hep-ph].
- [40] J. Alwall, et al., MadGraph 5: going beyond, *J. High Energy Phys.* 1106 (2011) 128, arXiv:1106.0522 [hep-ph].
- [41] ATLAS Collaboration, Electron reconstruction and identification efficiency measurements with the ATLAS detector using the 2011 LHC proton–proton collision data, *Eur. Phys. J. C* 74 (2014) 2941, arXiv:1404.2240 [hep-ex].
- [42] ATLAS Collaboration, Electron efficiency measurements with the ATLAS detector using the 2012 LHC proton–proton collision data, ATLAS-CONF-2014-032, <http://cdsweb.cern.ch/record/1706245>, 2014.
- [43] ATLAS Collaboration, Muon reconstruction performance of the ATLAS detector in proton–proton collision data at $\sqrt{s} = 13$ TeV, arXiv:1603.05598 [hep-ex], 2016.
- [44] M. Cacciari, G.P. Salam, Dispelling the N^3 myth for the k_t jet-finder, *Phys. Lett. B* 641 (2006) 57, arXiv:hep-ph/0512210.
- [45] M. Cacciari, G.P. Salam, G. Soyez, The anti- k_t jet clustering algorithm, *J. High Energy Phys.* 0804 (2008) 063, arXiv:0802.1189 [hep-ph].
- [46] ATLAS Collaboration, Performance of pile-up mitigation techniques for jets in pp collisions at $\sqrt{s} = 8$ TeV using the ATLAS detector, arXiv:1510.03823 [hep-ex], 2015.
- [47] ATLAS Collaboration, Expected performance of the ATLAS b-tagging algorithms in Run-2, ATLAS-PHYS-PUB-2015-022, <http://cdsweb.cern.ch/record/2037697>, 2015.
- [48] ATLAS Collaboration, Measurement of total and differential W^+W^- production cross sections in proton–proton collisions at $\sqrt{s} = 8$ TeV with the ATLAS detector and limits on anomalous triple-gauge-boson couplings, arXiv:1603.01702 [hep-ex], 2016.
- [49] N. Kidonakis, Two-loop soft anomalous dimensions for single top quark associated production with a W^- or H^- , *Phys. Rev. D* 82 (2010) 054018, arXiv:1005.4451 [hep-ph].
- [50] R.D. Ball, et al., Parton distributions for the LHC Run II, *J. High Energy Phys.* 04 (2015) 040, arXiv:1410.8849 [hep-ph].
- [51] J. Butterworth, et al., PDF4LHC recommendations for LHC Run II, *J. Phys. G, Nucl. Part. Phys.* 43 (2016) 023001, arXiv:1510.03865 [hep-ph].
- [52] J.M. Campbell, R.K. Ellis, An update on vector boson pair production at hadron colliders, *Phys. Rev. D* 60 (1999) 113006, arXiv:hep-ph/9905386.
- [53] ATLAS Collaboration, Jet Calibration and Systematic Uncertainties for Jets Reconstructed in the ATLAS Detector at $\sqrt{s} = 13$ TeV, ATLAS-PHYS-PUB-2015-015, <http://cdsweb.cern.ch/record/2037613>, 2015.
- [54] ATLAS Collaboration, Improved luminosity determination in pp collisions at $\sqrt{s} = 7$ TeV using the ATLAS detector at the LHC, *Eur. Phys. J. C* 73 (2013) 2518, arXiv:1302.4393 [hep-ex].
- [55] J. Wenninger, Energy Calibration of the LHC Beams at 4 TeV, CERN-ATS-2013-040, <http://cdsweb.cern.ch/record/1546734>, 2013.
- [56] CMS Collaboration, Measurement of the top quark pair production cross section in proton–proton collisions at $\sqrt{s} = 13$ TeV, *Phys. Rev. Lett.* 116 (2016) 052002, arXiv:1510.05302 [hep-ex].
- [57] ATLAS Collaboration, ATLAS Computing Acknowledgements 2016–2017, ATLAS-PHYS-PUB-2016-002, <http://cdsweb.cern.ch/record/2202407>, 2016.

ATLAS Collaboration

M. Aaboud^{136d}, G. Aad⁸⁷, B. Abbott¹¹⁴, J. Abdallah⁶⁵, O. Abdinov¹², B. Abeloos¹¹⁸, R. Aben¹⁰⁸, O.S. AbouZeid¹³⁸, N.L. Abraham¹⁵⁰, H. Abramowicz¹⁵⁴, H. Abreu¹⁵³, R. Abreu¹¹⁷, Y. Abulaiti^{147a,147b}, B.S. Acharya^{164a,164b,1}, L. Adamczyk^{40a}, D.L. Adams²⁷, J. Adelman¹⁰⁹, S. Adomeit¹⁰¹, T. Adye¹³², A.A. Affolder⁷⁶, T. Agatonovic-Jovin¹⁴, J. Agricola⁵⁶, J.A. Aguilar-Saavedra^{127a,127f}, S.P. Ahlen²⁴, F. Ahmadov^{67,2}, G. Aielli^{134a,134b}, H. Akerstedt^{147a,147b}, T.P.A. Åkesson⁸³, A.V. Akimov⁹⁷, G.L. Alberghi^{22a,22b}, J. Albert¹⁶⁹, S. Albrand⁵⁷, M.J. Alconada Verzini⁷³, M. Aleksa³², I.N. Aleksandrov⁶⁷, C. Alexa^{28b}, G. Alexander¹⁵⁴, T. Alexopoulos¹⁰, M. Alhroob¹¹⁴, B. Ali¹²⁹, M. Aliev^{75a,75b}, G. Alimonti^{93a}, J. Alison³³, S.P. Alkire³⁷, B.M.M. Allbrooke¹⁵⁰, B.W. Allen¹¹⁷, P.P. Allport¹⁹, A. Aloisio^{105a,105b}, A. Alonso³⁸, F. Alonso⁷³, C. Alpigiani¹³⁹, M. Alstamy⁸⁷, B. Alvarez Gonzalez³², D. Álvarez Piqueras¹⁶⁷, M.G. Alviggi^{105a,105b}, B.T. Amadio¹⁶, K. Amako⁶⁸, Y. Amaral Coutinho^{26a}, C. Amelung²⁵, D. Amidei⁹¹, S.P. Amor Dos Santos^{127a,127c}, A. Amorim^{127a,127b}, S. Amoroso³², G. Amundsen²⁵, C. Anastopoulos¹⁴⁰, L.S. Ancu⁵¹, N. Andari¹⁰⁹, T. Andeen¹¹, C.F. Anders^{60b}, G. Anders³², J.K. Anders⁷⁶, K.J. Anderson³³, A. Andreazza^{93a,93b}, V. Andrei^{60a}, S. Angelidakis⁹, I. Angelozzi¹⁰⁸, P. Anger⁴⁶, A. Angerami³⁷, F. Anghinolfi³², A.V. Anisenkov^{110,3}, N. Anjos¹³, A. Annovi^{125a,125b}, C. Antel^{60a}, M. Antonelli⁴⁹, A. Antonov^{99,*}, F. Anulli^{133a}, M. Aoki⁶⁸, L. Aperio Bella¹⁹, G. Arabidze⁹², Y. Arai⁶⁸, J.P. Araque^{127a}, A.T.H. Arce⁴⁷, F.A. Arduh⁷³, J-F. Arguin⁹⁶, S. Argyropoulos⁶⁵, M. Arik^{20a}, A.J. Armbruster¹⁴⁴, L.J. Armitage⁷⁸, O. Arnaez³², H. Arnold⁵⁰, M. Arratia³⁰, O. Arslan²³, A. Artamonov⁹⁸, G. Artoni¹²¹, S. Artz⁸⁵, S. Asai¹⁵⁶, N. Asbah⁴⁴, A. Ashkenazi¹⁵⁴, B. Åsman^{147a,147b}, L. Asquith¹⁵⁰, K. Assamagan²⁷, R. Astalos^{145a}, M. Atkinson¹⁶⁶, N.B. Atlay¹⁴², K. Augsten¹²⁹, G. Avolio³², B. Axen¹⁶, M.K. Ayoub¹¹⁸, G. Azuelos^{96,4}, M.A. Baak³², A.E. Baas^{60a}, M.J. Baca¹⁹, H. Bachacou¹³⁷, K. Bachas^{75a,75b}, M. Backes³², M. Backhaus³², P. Bagiachi^{133a,133b}, P. Bagnaia^{133a,133b}, Y. Bai^{35a}, J.T. Baines¹³², O.K. Baker¹⁷⁶, E.M. Baldin^{110,3}, P. Balek¹³⁰, T. Balestri¹⁴⁹, F. Balli¹³⁷, W.K. Balunas¹²³, E. Banas⁴¹, Sw. Banerjee^{173,5}, A.A.E. Bannoura¹⁷⁵, L. Barak³², E.L. Barberio⁹⁰, D. Barberis^{52a,52b}, M. Barbero⁸⁷, T. Barillari¹⁰², T. Barklow¹⁴⁴, N. Barlow³⁰, S.L. Barnes⁸⁶, B.M. Barnett¹³², R.M. Barnett¹⁶, Z. Barnovska⁵, A. Baroncelli^{135a}, G. Barone²⁵, A.J. Barr¹²¹, L. Barranco Navarro¹⁶⁷, F. Barreiro⁸⁴, J. Barreiro Guimarães da Costa^{35a}, R. Bartoldus¹⁴⁴, A.E. Barton⁷⁴, P. Bartos^{145a}, A. Basalae¹²⁴, A. Bassalat¹¹⁸, R.L. Bates⁵⁵, S.J. Batista¹⁵⁹, J.R. Batley³⁰, M. Battaglia¹³⁸, M. Baue^{133a,133b}, F. Bauer¹³⁷, H.S. Bawa^{144,6}, J.B. Beacham¹¹², M.D. Beattie⁷⁴, T. Beau⁸², P.H. Beauchemin¹⁶², P. Bechtel²³, H.P. Beck^{18,7}, K. Becker¹²¹, M. Becker⁸⁵, M. Beckingham¹⁷⁰, C. Becot¹¹¹, A.J. Beddall^{20e}, A. Beddall^{20b}, V.A. Bednyakov⁶⁷, M. Bedognetti¹⁰⁸, C.P. Bee¹⁴⁹, L.J. Beemster¹⁰⁸, T.A. Beermann³², M. Beger²⁷, J.K. Behr⁴⁴, C. Belanger-Champagne⁸⁹, A.S. Bell⁸⁰, G. Bella¹⁵⁴, L. Bellagamba^{22a}, A. Bellerive³¹, M. Bellomo⁸⁸, K. Belotskiy⁹⁹, O. Beltramello³², N.L. Belyaev⁹⁹, O. Benary¹⁵⁴, D. Bencheikroun^{136a}, M. Bender¹⁰¹, K. Bendtz^{147a,147b}, N. Benekos¹⁰, Y. Benhammou¹⁵⁴, E. Benhar Noccioli¹⁷⁶, J. Benitez⁶⁵, D.P. Benjamin⁴⁷, J.R. Bensinger²⁵, S. Bentvelsen¹⁰⁸, L. Beresford¹²¹, M. Beretta⁴⁹, D. Berge¹⁰⁸, E. Bergeaas Kuutmann¹⁶⁵, N. Berger⁵, J. Beringer¹⁶, S. Berlendis⁵⁷, N.R. Bernard⁸⁸, C. Bernius¹¹¹, F.U. Bernlochner²³, T. Berry⁷⁹, P. Berta¹³⁰, C. Bertella⁸⁵, G. Bertoli^{147a,147b}, F. Bertolucci^{125a,125b}, I.A. Bertram⁷⁴, C. Bertsche⁴⁴, D. Bertsche¹¹⁴, G.J. Besjes³⁸, O. Bessidskaia Bylund^{147a,147b}, M. Bessner⁴⁴, N. Besson¹³⁷, C. Betancourt⁵⁰, S. Bethke¹⁰², A.J. Bevan⁷⁸, W. Bhimji¹⁶, R.M. Bianchi¹²⁶, L. Bianchini²⁵, M. Bianco³², O. Biebel¹⁰¹, D. Biedermann¹⁷, R. Bielski⁸⁶, N.V. Biesuz^{125a,125b}, M. Biglietti^{135a}, J. Bilbao De Mendizabal⁵¹, H. Bilokon⁴⁹, M. Bindi⁵⁶, S. Binet¹¹⁸, A. Bingul^{20b}, C. Bini^{133a,133b}, S. Biondi^{22a,22b}, D.M. Bjergaard⁴⁷, C.W. Black¹⁵¹, J.E. Black¹⁴⁴, K.M. Black²⁴, D. Blackburn¹³⁹, R.E. Blair⁶, J.-B. Blanchard¹³⁷, J.E. Blanco⁷⁹, T. Blazek^{145a}, I. Bloch⁴⁴, C. Blocker²⁵, W. Blum^{85,*}, U. Blumenschein⁵⁶, S. Blunier^{34a}, G.J. Bobbink¹⁰⁸, V.S. Bobrovnikov^{110,3}, S.S. Bocchetta⁸³, A. Bocci⁴⁷, C. Bock¹⁰¹, M. Boehler⁵⁰, D. Boerner¹⁷⁵, J.A. Bogaerts³², D. Bogavac¹⁴, A.G. Bogdanchikov¹¹⁰, C. Bohm^{147a}, V. Boisvert⁷⁹, P. Bokan¹⁴, T. Bold^{40a}, A.S. Boldyrev^{164a,164c}, M. Bomben⁸², M. Bona⁷⁸, M. Boonekamp¹³⁷, A. Borisov¹³¹, G. Borissov⁷⁴, J. Bortfeldt³², D. Bortoletto¹²¹, V. Bortolotto^{62a,62b,62c}, K. Bos¹⁰⁸, D. Boscherini^{22a}, M. Bosman¹³, J.D. Bossio Sola²⁹, J. Boudreau¹²⁶, J. Bouffard², E.V. Bouhova-Thacker⁷⁴, D. Boumediene³⁶, C. Bourdarios¹¹⁸, S.K. Boutle⁵⁵, A. Boveia³², J. Boyd³², I.R. Boyko⁶⁷, J. Bracinik¹⁹, A. Brandt⁸, G. Brandt⁵⁶, O. Brandt^{60a}, U. Bratzler¹⁵⁷, B. Brau⁸⁸, J.E. Brau¹¹⁷, H.M. Braun^{175,*}, W.D. Breaden Madden⁵⁵, K. Brendlinger¹²³, A.J. Brennan⁹⁰, L. Brenner¹⁰⁸, R. Brenner¹⁶⁵, S. Bressler¹⁷², T.M. Bristow⁴⁸, D. Britton⁵⁵, D. Britzger⁴⁴, F.M. Brochu³⁰, I. Brock²³,

R. Brock⁹², G. Brooijmans³⁷, T. Brooks⁷⁹, W.K. Brooks^{34b}, J. Brosamer¹⁶, E. Brost¹¹⁷, J.H. Broughton¹⁹, P.A. Bruckman de Renstrom⁴¹, D. Bruncko^{145b}, R. Bruneliere⁵⁰, A. Bruni^{22a}, G. Bruni^{22a}, L.S. Bruni¹⁰⁸, B.H. Brunt³⁰, M. Bruschi^{22a}, N. Bruscinio²³, P. Bryant³³, L. Bryngemark⁸³, T. Buanes¹⁵, Q. Buat¹⁴³, P. Buchholz¹⁴², A.G. Buckley⁵⁵, I.A. Budagov⁶⁷, F. Buehrer⁵⁰, M.K. Bugge¹²⁰, O. Bulekov⁹⁹, D. Bullock⁸, H. Burckhart³², S. Burdin⁷⁶, C.D. Burgard⁵⁰, B. Burghgrave¹⁰⁹, K. Burka⁴¹, S. Burke¹³², I. Burmeister⁴⁵, J.T.P. Burr¹²¹, E. Busato³⁶, D. Büscher⁵⁰, V. Büscher⁸⁵, P. Bussey⁵⁵, J.M. Butler²⁴, C.M. Buttar⁵⁵, J.M. Butterworth⁸⁰, P. Butti¹⁰⁸, W. Buttinger²⁷, A. Buzatu⁵⁵, A.R. Buzykaev^{110,3}, S. Cabrera Urbán¹⁶⁷, D. Caforio¹²⁹, V.M. Cairo^{39a,39b}, O. Cakir^{4a}, N. Calace⁵¹, P. Calafiura¹⁶, A. Calandri⁸⁷, G. Calderini⁸², P. Calfayan¹⁰¹, L.P. Caloba^{26a}, D. Calvet³⁶, S. Calvet³⁶, T.P. Calvet⁸⁷, R. Camacho Toro³³, S. Camarda³², P. Camarri^{134a,134b}, D. Cameron¹²⁰, R. Caminal Armadans¹⁶⁶, C. Camincher⁵⁷, S. Campana³², M. Campanelli⁸⁰, A. Camplani^{93a,93b}, A. Campoverde¹⁴², V. Canale^{105a,105b}, A. Canepa^{160a}, M. Cano Bret^{35e}, J. Cantero¹¹⁵, R. Cantrill^{127a}, T. Cao⁴², M.D.M. Capeans Garrido³², I. Caprini^{28b}, M. Caprini^{28b}, M. Capua^{39a,39b}, R. Caputo⁸⁵, R.M. Carbone³⁷, R. Cardarelli^{134a}, F. Cardillo⁵⁰, I. Carli¹³⁰, T. Carli³², G. Carlino^{105a}, L. Carminati^{93a,93b}, S. Caron¹⁰⁷, E. Carquin^{34b}, G.D. Carrillo-Montoya³², J.R. Carter³⁰, J. Carvalho^{127a,127c}, D. Casadei¹⁹, M.P. Casado^{13,8}, M. Casolino¹³, D.W. Casper¹⁶³, E. Castaneda-Miranda^{146a}, R. Castelijin¹⁰⁸, A. Castelli¹⁰⁸, V. Castillo Gimenez¹⁶⁷, N.F. Castro^{127a,9}, A. Catinaccio³², J.R. Catmore¹²⁰, A. Cattai³², J. Caudron⁸⁵, V. Cavaliere¹⁶⁶, E. Cavallaro¹³, D. Cavalli^{93a}, M. Cavalli-Sforza¹³, V. Cavasinni^{125a,125b}, F. Ceradini^{135a,135b}, L. Cerda Alberich¹⁶⁷, B.C. Cerio⁴⁷, A.S. Cerqueira^{26b}, A. Cerri¹⁵⁰, L. Cerrito⁷⁸, F. Cerutti¹⁶, M. Cerv³², A. Cervelli¹⁸, S.A. Cetin^{20d}, A. Chafaq^{136a}, D. Chakraborty¹⁰⁹, S.K. Chan⁵⁹, Y.L. Chan^{62a}, P. Chang¹⁶⁶, J.D. Chapman³⁰, D.G. Charlton¹⁹, A. Chatterjee⁵¹, C.C. Chau¹⁵⁹, C.A. Chavez Barajas¹⁵⁰, S. Che¹¹², S. Cheatham⁷⁴, A. Chegwidden⁹², S. Chekanov⁶, S.V. Chekulaev^{160a}, G.A. Chelkov^{67,10}, M.A. Chelstowska⁹¹, C. Chen⁶⁶, H. Chen²⁷, K. Chen¹⁴⁹, S. Chen^{35c}, S. Chen¹⁵⁶, X. Chen^{35f}, Y. Chen⁶⁹, H.C. Cheng⁹¹, H.J. Cheng^{35a}, Y. Cheng³³, A. Cheplakov⁶⁷, E. Cheremushkina¹³¹, R. Cherkaoui El Moursli^{136e}, V. Chernyatin^{27,*}, E. Cheu⁷, L. Chevalier¹³⁷, V. Chiarella⁴⁹, G. Chiarelli^{125a,125b}, G. Chiodini^{75a}, A.S. Chisholm¹⁹, A. Chitan^{28b}, M.V. Chizhov⁶⁷, K. Choi⁶³, A.R. Chomont³⁶, S. Chouridou⁹, B.K.B. Chow¹⁰¹, V. Christodoulou⁸⁰, D. Chromek-Burckhart³², J. Chudoba¹²⁸, A.J. Chuinard⁸⁹, J.J. Chwastowski⁴¹, L. Chytka¹¹⁶, G. Ciapetti^{133a,133b}, A.K. Ciftci^{4a}, D. Cinca⁴⁵, V. Cindro⁷⁷, I.A. Cioara²³, A. Ciochio¹⁶, F. Ciotto^{105a,105b}, Z.H. Citron¹⁷², M. Citterio^{93a}, M. Ciubancan^{28b}, A. Clark⁵¹, B.L. Clark⁵⁹, M.R. Clark³⁷, P.J. Clark⁴⁸, R.N. Clarke¹⁶, C. Clement^{147a,147b}, Y. Coadou⁸⁷, M. Cobal^{164a,164c}, A. Coccaro⁵¹, J. Cochran⁶⁶, L. Coffey²⁵, L. Colasurdo¹⁰⁷, B. Cole³⁷, A.P. Colijn¹⁰⁸, J. Collot⁵⁷, T. Colombo³², G. Compostella¹⁰², P. Conde Muiño^{127a,127b}, E. Coniavitis⁵⁰, S.H. Connell^{146b}, I.A. Connelly⁷⁹, V. Consorti⁵⁰, S. Constantinescu^{28b}, G. Conti³², F. Conventi^{105a,11}, M. Cooke¹⁶, B.D. Cooper⁸⁰, A.M. Cooper-Sarkar¹²¹, K.J.R. Cormier¹⁵⁹, T. Cornelissen¹⁷⁵, M. Corradi^{133a,133b}, F. Corriveau^{89,12}, A. Corso-Radu¹⁶³, A. Cortes-Gonzalez¹³, G. Cortiana¹⁰², G. Costa^{93a}, M.J. Costa¹⁶⁷, D. Costanzo¹⁴⁰, G. Cottin³⁰, G. Cowan⁷⁹, B.E. Cox⁸⁶, K. Cranmer¹¹¹, S.J. Crawley⁵⁵, G. Cree³¹, S. Crépe-Renaudin⁵⁷, F. Crescioli⁸², W.A. Cribbs^{147a,147b}, M. Crispin Ortuzar¹²¹, M. Cristinziani²³, V. Croft¹⁰⁷, G. Crosetti^{39a,39b}, T. Cuhadar Donszelmann¹⁴⁰, J. Cummings¹⁷⁶, M. Curatolo⁴⁹, J. Cúth⁸⁵, C. Cuthbert¹⁵¹, H. Czirr¹⁴², P. Czodrowski³, G. D'amen^{22a,22b}, S. D'Auria⁵⁵, M. D'Onofrio⁷⁶, M.J. Da Cunha Sargedass De Sousa^{127a,127b}, C. Da Via⁸⁶, W. Dabrowski^{40a}, T. Dado^{145a}, T. Dai⁹¹, O. Dale¹⁵, F. Dallaire⁹⁶, C. Dallapiccola⁸⁸, M. Dam³⁸, J.R. Dandoy³³, N.P. Dang⁵⁰, A.C. Daniells¹⁹, N.S. Dann⁸⁶, M. Danninger¹⁶⁸, M. Dano Hoffmann¹³⁷, V. Dao⁵⁰, G. Darbo^{52a}, S. Darmora⁸, J. Dassoulas³, A. Dattagupta⁶³, W. Davey²³, C. David¹⁶⁹, T. Davidek¹³⁰, M. Davies¹⁵⁴, P. Davison⁸⁰, E. Dawe⁹⁰, I. Dawson¹⁴⁰, R.K. Daya-Ishmukhametova⁸⁸, K. De⁸, R. de Asmundis^{105a}, A. De Benedetti¹¹⁴, S. De Castro^{22a,22b}, S. De Cecco⁸², N. De Groot¹⁰⁷, P. de Jong¹⁰⁸, H. De la Torre⁸⁴, F. De Lorenzi⁶⁶, A. De Maria⁵⁶, D. De Pedis^{133a}, A. De Salvo^{133a}, U. De Sanctis¹⁵⁰, A. De Santo¹⁵⁰, J.B. De Vivie De Regie¹¹⁸, W.J. Dearnaley⁷⁴, R. Debbe²⁷, C. Debenedetti¹³⁸, D.V. Dedovich⁶⁷, N. Dehghanian³, I. Deigaard¹⁰⁸, M. Del Gaudio^{39a,39b}, J. Del Peso⁸⁴, T. Del Prete^{125a,125b}, D. Delgove¹¹⁸, F. Deliot¹³⁷, C.M. Delitzsch⁵¹, M. Deliyergiyev⁷⁷, A. Dell'Acqua³², L. Dell'Asta²⁴, M. Dell'Orso^{125a,125b}, M. Della Pietra^{105a,11}, D. della Volpe⁵¹, M. Delmastro⁵, P.A. Delsart⁵⁷, D.A. DeMarco¹⁵⁹, S. Demers¹⁷⁶, M. Demichev⁶⁷, A. Demilly⁸², S.P. Denisov¹³¹, D. Denysiuk¹³⁷, D. Derendarz⁴¹, J.E. Derkaoui^{136d}, F. Derue⁸², P. Dervan⁷⁶, K. Desch²³, C. Deterre⁴⁴, K. Dette⁴⁵, P.O. Deviveiros³², A. Dewhurst¹³²,

S. Dhaliwal²⁵, A. Di Ciaccio^{134a,134b}, L. Di Ciaccio⁵, W.K. Di Clemente¹²³, C. Di Donato^{133a,133b}, A. Di Girolamo³², B. Di Girolamo³², B. Di Micco^{135a,135b}, R. Di Nardo³², A. Di Simone⁵⁰, R. Di Sipio¹⁵⁹, D. Di Valentino³¹, C. Diaconu⁸⁷, M. Diamond¹⁵⁹, F.A. Dias⁴⁸, M.A. Diaz^{34a}, E.B. Diehl⁹¹, J. Dietrich¹⁷, S. Diglio⁸⁷, A. Dimitrievska¹⁴, J. Dingfelder²³, P. Dita^{28b}, S. Dita^{28b}, F. Dittus³², F. Djama⁸⁷, T. Djobava^{53b}, J.I. Djuvsland^{60a}, M.A.B. do Vale^{26c}, D. Dobos³², M. Dobre^{28b}, C. Doglioni⁸³, T. Dohmae¹⁵⁶, J. Dolejsi¹³⁰, Z. Dolezal¹³⁰, B.A. Dolgoshein^{99,*}, M. Donadelli^{26d}, S. Donati^{125a,125b}, P. Dondero^{122a,122b}, J. Donini³⁶, J. Dopke¹³², A. Doria^{105a}, M.T. Dova⁷³, A.T. Doyle⁵⁵, E. Drechsler⁵⁶, M. Dris¹⁰, Y. Du^{35d}, J. Duarte-Campderros¹⁵⁴, E. Duchovni¹⁷², G. Duckeck¹⁰¹, O.A. Ducu^{96,13}, D. Duda¹⁰⁸, A. Dudarev³², E.M. Duffield¹⁶, L. Dufлот¹¹⁸, L. Duguid⁷⁹, M. Dührssen³², M. Dumancic¹⁷², M. Dunford^{60a}, H. Duran Yildiz^{4a}, M. Düren⁵⁴, A. Durglishvili^{53b}, D. Duschinger⁴⁶, B. Dutta⁴⁴, M. Dyndal⁴⁴, C. Eckardt⁴⁴, K.M. Ecker¹⁰², R.C. Edgar⁹¹, N.C. Edwards⁴⁸, T. Eifert³², G. Eigen¹⁵, K. Einsweiler¹⁶, T. Ekelof¹⁶⁵, M. El Kacimi^{136c}, V. Ellajosyula⁸⁷, M. Ellert¹⁶⁵, S. Elles⁵, F. Ellinghaus¹⁷⁵, A.A. Elliot¹⁶⁹, N. Ellis³², J. Elmsheuser²⁷, M. Elsing³², D. Emeliyanov¹³², Y. Enari¹⁵⁶, O.C. Endner⁸⁵, M. Endo¹¹⁹, J.S. Ennis¹⁷⁰, J. Erdmann⁴⁵, A. Ereditato¹⁸, G. Ernis¹⁷⁵, J. Ernst², M. Ernst²⁷, S. Errede¹⁶⁶, E. Ertel⁸⁵, M. Escalier¹¹⁸, H. Esch⁴⁵, C. Escobar¹²⁶, B. Esposito⁴⁹, A.I. Etienvre¹³⁷, E. Etzion¹⁵⁴, H. Evans⁶³, A. Ezhilov¹²⁴, F. Fabbri^{22a,22b}, L. Fabbri^{22a,22b}, G. Facini³³, R.M. Fakhruddinov¹³¹, S. Falciano^{133a}, R.J. Falla⁸⁰, J. Faltova³², Y. Fang^{35a}, M. Fanti^{93a,93b}, A. Farbin⁸, A. Farilla^{135a}, C. Farina¹²⁶, T. Farooque¹³, S. Farrell¹⁶, S.M. Farrington¹⁷⁰, P. Farthouat³², F. Fassi^{136e}, P. Fassnacht³², D. Fassoulotis⁹, M. Fauci Giannelli⁷⁹, A. Favareto^{52a,52b}, W.J. Fawcett¹²¹, L. Fayard¹¹⁸, O.L. Fedin^{124,14}, W. Fedorko¹⁶⁸, S. Feigl¹²⁰, L. Feligioni⁸⁷, C. Feng^{35d}, E.J. Feng³², H. Feng⁹¹, A.B. Fenyuk¹³¹, L. Feremenga⁸, P. Fernandez Martinez¹⁶⁷, S. Fernandez Perez¹³, J. Ferrando⁵⁵, A. Ferrari¹⁶⁵, P. Ferrari¹⁰⁸, R. Ferrari^{122a}, D.E. Ferreira de Lima^{60b}, A. Ferrer¹⁶⁷, D. Ferrere⁵¹, C. Ferretti⁹¹, A. Ferretto Parodi^{52a,52b}, F. Fiedler⁸⁵, A. Filipčič⁷⁷, M. Filipuzzi⁴⁴, F. Filthaut¹⁰⁷, M. Fincke-Keeler¹⁶⁹, K.D. Finelli¹⁵¹, M.C.N. Fiolhais^{127a,127c}, L. Fiorini¹⁶⁷, A. Firan⁴², A. Fischer², C. Fischer¹³, J. Fischer¹⁷⁵, W.C. Fisher⁹², N. Flaschel⁴⁴, I. Fleck¹⁴², P. Fleischmann⁹¹, G.T. Fletcher¹⁴⁰, R.R.M. Fletcher¹²³, T. Flick¹⁷⁵, A. Floderus⁸³, L.R. Flores Castillo^{62a}, M.J. Flowerdew¹⁰², G.T. Forcolin⁸⁶, A. Formica¹³⁷, A. Forti⁸⁶, A.G. Foster¹⁹, D. Fournier¹¹⁸, H. Fox⁷⁴, S. Fracchia¹³, P. Francavilla⁸², M. Franchini^{22a,22b}, D. Francis³², L. Franconi¹²⁰, M. Franklin⁵⁹, M. Frate¹⁶³, M. Fraternali^{122a,122b}, D. Freeborn⁸⁰, S.M. Fressard-Batraneanu³², F. Friedrich⁴⁶, D. Froidevaux³², J.A. Frost¹²¹, C. Fukunaga¹⁵⁷, E. Fullana Torregrosa⁸⁵, T. Fusayasu¹⁰³, J. Fuster¹⁶⁷, C. Gabaldon⁵⁷, O. Gabizon¹⁷⁵, A. Gabrielli^{22a,22b}, A. Gabrielli¹⁶, G.P. Gach^{40a}, S. Gadatsch³², S. Gadomski⁵¹, G. Gagliardi^{52a,52b}, L.G. Gagnon⁹⁶, P. Gagnon⁶³, C. Galea¹⁰⁷, B. Galhardo^{127a,127c}, E.J. Gallas¹²¹, B.J. Gallop¹³², P. Gallus¹²⁹, G. Galster³⁸, K.K. Gan¹¹², J. Gao^{35b}, Y. Gao⁴⁸, Y.S. Gao^{144,6}, F.M. Garay Walls⁴⁸, C. García¹⁶⁷, J.E. García Navarro¹⁶⁷, M. Garcia-Sciveres¹⁶, R.W. Gardner³³, N. Garelli¹⁴⁴, V. Garonne¹²⁰, A. Gascon Bravo⁴⁴, C. Gatti⁴⁹, A. Gaudiello^{52a,52b}, G. Gaudio^{122a}, B. Gaur¹⁴², L. Gauthier⁹⁶, I.L. Gavrilenko⁹⁷, C. Gay¹⁶⁸, G. Gaycken²³, E.N. Gazis¹⁰, Z. Gecse¹⁶⁸, C.N.P. Gee¹³², Ch. Geich-Gimbel²³, M. Geisen⁸⁵, M.P. Geisler^{60a}, C. Gemme^{52a}, M.H. Genest⁵⁷, C. Geng^{35b,15}, S. Gentile^{133a,133b}, S. George⁷⁹, D. Gerbaudo¹³, A. Gershon¹⁵⁴, S. Ghasemi¹⁴², H. Ghazlane^{136b}, M. Ghneimat²³, B. Giacobbe^{22a}, S. Giagu^{133a,133b}, P. Giannetti^{125a,125b}, B. Gibbard²⁷, S.M. Gibson⁷⁹, M. Gignac¹⁶⁸, M. Gilchriese¹⁶, T.P.S. Gillam³⁰, D. Gillberg³¹, G. Gilles¹⁷⁵, D.M. Gingrich^{3,4}, N. Giokaris⁹, M.P. Giordani^{164a,164c}, F.M. Giorgi^{22a}, F.M. Giorgi¹⁷, P.F. Giraud¹³⁷, P. Giromini⁵⁹, D. Giugni^{93a}, F. Giuli¹²¹, C. Giuliani¹⁰², M. Giulini^{60b}, B.K. Gjelsten¹²⁰, S. Gkaitatzis¹⁵⁵, I. Gkialas¹⁵⁵, E.L. Gkougkousis¹¹⁸, L.K. Gladilin¹⁰⁰, C. Glasman⁸⁴, J. Glatzer⁵⁰, P.C.F. Glaysheer⁴⁸, A. Glazov⁴⁴, M. Goblirsch-Kolb¹⁰², J. Godlewski⁴¹, S. Goldfarb⁹⁰, T. Golling⁵¹, D. Golubkov¹³¹, A. Gomes^{127a,127b,127d}, R. Gonçalves^{127a}, J. Goncalves Pinto Firmino Da Costa¹³⁷, G. Gonella⁵⁰, L. Gonella¹⁹, A. Gongadze⁶⁷, S. González de la Hoz¹⁶⁷, G. Gonzalez Parra¹³, S. Gonzalez-Sevilla⁵¹, L. Goossens³², P.A. Gorbounov⁹⁸, H.A. Gordon²⁷, I. Gorelov¹⁰⁶, B. Gorini³², E. Gorini^{75a,75b}, A. Gorišek⁷⁷, E. Gornicki⁴¹, A.T. Goshaw⁴⁷, C. Gössling⁴⁵, M.I. Gostkin⁶⁷, C.R. Goudet¹¹⁸, D. Goujdami^{136c}, A.G. Goussiou¹³⁹, N. Govender^{146b,16}, E. Gozani¹⁵³, L. Graber⁵⁶, I. Grabowska-Bold^{40a}, P.O.J. Gradin⁵⁷, P. Grafström^{22a,22b}, J. Gramling⁵¹, E. Gramstad¹²⁰, S. Grancagnolo¹⁷, V. Gratchev¹²⁴, P.M. Gravila^{28e}, H.M. Gray³², E. Graziani^{135a}, Z.D. Greenwood^{81,17}, C. Grefe²³, K. Gregersen⁸⁰, I.M. Gregor⁴⁴, P. Grenier¹⁴⁴, K. Grevtsov⁵, J. Griffiths⁸, A.A. Grillo¹³⁸, K. Grimm⁷⁴, S. Grinstein^{13,18}, Ph. Gris³⁶, J.-F. Grivaz¹¹⁸, S. Groh⁸⁵, J.P. Grohs⁴⁶, E. Gross¹⁷², J. Grosse-Knetter⁵⁶, G.C. Grossi⁸¹,

Z.J. Grout¹⁵⁰, L. Guan⁹¹, W. Guan¹⁷³, J. Guenther⁶⁴, F. Guescini⁵¹, D. Guest¹⁶³, O. Gueta¹⁵⁴, E. Guido^{52a,52b}, T. Guillemin⁵, S. Guindon², U. Gul⁵⁵, C. Gumpert³², J. Guo^{35e}, Y. Guo^{35b,15}, S. Gupta¹²¹, G. Gustavino^{133a,133b}, P. Gutierrez¹¹⁴, N.G. Gutierrez Ortiz⁸⁰, C. Gutsche⁴⁶, C. Guyot¹³⁷, C. Gwenlan¹²¹, C.B. Gwilliam⁷⁶, A. Haas¹¹¹, C. Haber¹⁶, H.K. Hadavand⁸, N. Haddad^{136e}, A. Hadeef⁸⁷, P. Haefner²³, S. Hageböck²³, Z. Hajduk⁴¹, H. Hakobyan^{177,*}, M. Haleem⁴⁴, J. Haley¹¹⁵, G. Halladjian⁹², G.D. Hallowell⁸⁷, K. Hamacher¹⁷⁵, P. Hamal¹¹⁶, K. Hamano¹⁶⁹, A. Hamilton^{146a}, G.N. Hamity¹⁴⁰, P.G. Hamnett⁴⁴, L. Han^{35b}, K. Hanagaki^{68,19}, K. Hanawa¹⁵⁶, M. Hance¹³⁸, B. Haney¹²³, P. Hanke^{60a}, R. Hanna¹³⁷, J.B. Hansen³⁸, J.D. Hansen³⁸, M.C. Hansen²³, P.H. Hansen³⁸, K. Hara¹⁶¹, A.S. Hard¹⁷³, T. Harenberg¹⁷⁵, F. Hariri¹¹⁸, S. Harkusha⁹⁴, R.D. Harrington⁴⁸, P.F. Harrison¹⁷⁰, F. Hartjes¹⁰⁸, N.M. Hartmann¹⁰¹, M. Hasegawa⁶⁹, Y. Hasegawa¹⁴¹, A. Hasib¹¹⁴, S. Hassani¹³⁷, S. Haug¹⁸, R. Hauser⁹², L. Hauswald⁴⁶, M. Havranek¹²⁸, C.M. Hawkes¹⁹, R.J. Hawkes³², D. Hayden⁹², C.P. Hays¹²¹, J.M. Hays⁷⁸, H.S. Hayward⁷⁶, S.J. Haywood¹³², S.J. Head¹⁹, T. Heck⁸⁵, V. Hedberg⁸³, L. Heelan⁸, S. Heim¹²³, T. Heim¹⁶, B. Heinemann¹⁶, J.J. Heinrich¹⁰¹, L. Heinrich¹¹¹, C. Heinz⁵⁴, J. Hejbal¹²⁸, L. Helary²⁴, S. Hellman^{147a,147b}, C. Helsens³², J. Henderson¹²¹, R.C.W. Henderson⁷⁴, Y. Heng¹⁷³, S. Henkelmann¹⁶⁸, A.M. Henriques Correia³², S. Henrot-Versille¹¹⁸, G.H. Herbert¹⁷, Y. Hernández Jiménez¹⁶⁷, G. Herten⁵⁰, R. Hertenberger¹⁰¹, L. Hervas³², G.G. Hesketh⁸⁰, N.P. Hessey¹⁰⁸, J.W. Hetherly⁴², R. Hickling⁷⁸, E. Higón-Rodríguez¹⁶⁷, E. Hill¹⁶⁹, J.C. Hill³⁰, K.H. Hiller⁴⁴, S.J. Hillier¹⁹, I. Hinchliffe¹⁶, E. Hines¹²³, R.R. Hinman¹⁶, M. Hirose⁵⁰, D. Hirschbuehl¹⁷⁵, J. Hobbs¹⁴⁹, N. Hod^{160a}, M.C. Hodgkinson¹⁴⁰, P. Hodgson¹⁴⁰, A. Hoecker³², M.R. Hoefkamp¹⁰⁶, F. Hoenig¹⁰¹, D. Hohn²³, T.R. Holmes¹⁶, M. Homann⁴⁵, T.M. Hong¹²⁶, B.H. Hooberman¹⁶⁶, W.H. Hopkins¹¹⁷, Y. Horii¹⁰⁴, A.J. Horton¹⁴³, J.-Y. Hostachy⁵⁷, S. Hou¹⁵², A. Hoummada^{136a}, J. Howarth⁴⁴, M. Hrabovsky¹¹⁶, I. Hristova¹⁷, J. Hrivnac¹¹⁸, T. Hryn'ova⁵, A. Hrynevich⁹⁵, C. Hsu^{146c}, P.J. Hsu^{152,20}, S.-C. Hsu¹³⁹, D. Hu³⁷, Q. Hu^{35b}, Y. Huang⁴⁴, Z. Hubacek¹²⁹, F. Hubaut⁸⁷, F. Huegging²³, T.B. Huffman¹²¹, E.W. Hughes³⁷, G. Hughes⁷⁴, M. Huhtinen³², P. Huo¹⁴⁹, N. Huseynov^{67,2}, J. Huston⁹², J. Huth⁵⁹, G. Iacobucci⁵¹, G. Iakovidis²⁷, I. Ibragimov¹⁴², L. Iconomidou-Fayard¹¹⁸, E. Ideal¹⁷⁶, Z. Idrissi^{136e}, P. Iengo³², O. Igonkina^{108,21}, T. Iizawa¹⁷¹, Y. Ikegami⁶⁸, M. Ikeno⁶⁸, Y. Ilchenko^{11,22}, D. Iliadis¹⁵⁵, N. Ilic¹⁴⁴, T. Ince¹⁰², G. Introzzi^{122a,122b}, P. Ioannou^{9,*}, M. Iodice^{135a}, K. Iordanidou³⁷, V. Ippolito⁵⁹, M. Ishino⁷⁰, M. Ishitsuka¹⁵⁸, R. Ishmukhametov¹¹², C. Issever¹²¹, S. Istin^{20a}, F. Ito¹⁶¹, J.M. Iturbe Ponce⁸⁶, R. Iuppa^{134a,134b}, W. Iwanski⁶⁴, H. Iwasaki⁶⁸, J.M. Izen⁴³, V. Izzo^{105a}, S. Jabbar³, B. Jackson¹²³, M. Jackson⁷⁶, P. Jackson¹, V. Jain², K.B. Jakobi⁸⁵, K. Jakobs⁵⁰, S. Jakobsen³², T. Jakoubek¹²⁸, D.O. Jamin¹¹⁵, D.K. Jana⁸¹, E. Jansen⁸⁰, R. Jansky⁶⁴, J. Janssen²³, M. Janus⁵⁶, G. Jarlskog⁸³, N. Javadov^{67,2}, T. Javůrek⁵⁰, F. Jeanneau¹³⁷, L. Jeanty¹⁶, G.-Y. Jeng¹⁵¹, D. Jennens⁹⁰, P. Jenni^{50,23}, J. Jentzsch⁴⁵, C. Jeske¹⁷⁰, S. Jézéquel⁵, H. Ji¹⁷³, J. Jia¹⁴⁹, H. Jiang⁶⁶, Y. Jiang^{35b}, S. Jiggins⁸⁰, J. Jimenez Pena¹⁶⁷, S. Jin^{35a}, A. Jinaru^{28b}, O. Jinnouchi¹⁵⁸, P. Johansson¹⁴⁰, K.A. Johns⁷, W.J. Johnson¹³⁹, K. Jon-And^{147a,147b}, G. Jones¹⁷⁰, R.W.L. Jones⁷⁴, S. Jones⁷, T.J. Jones⁷⁶, J. Jongmanns^{60a}, P.M. Jorge^{127a,127b}, J. Jovicevic^{160a}, X. Ju¹⁷³, A. Juste Rozas^{13,18}, M.K. Köhler¹⁷², A. Kaczmarek⁴¹, M. Kado¹¹⁸, H. Kagan¹¹², M. Kagan¹⁴⁴, S.J. Kahn⁸⁷, E. Kajomovitz⁴⁷, C.W. Kalderon¹²¹, A. Kaluza⁸⁵, S. Kama⁴², A. Kamenshchikov¹³¹, N. Kanaya¹⁵⁶, S. Kaneti³⁰, L. Kanjir⁷⁷, V.A. Kantserov⁹⁹, J. Kanzaki⁶⁸, B. Kaplan¹¹¹, L.S. Kaplan¹⁷³, A. Kapliy³³, D. Kar^{146c}, K. Karakostas¹⁰, A. Karamaoun³, N. Karastathis¹⁰, M.J. Kareem⁵⁶, E. Karentzos¹⁰, M. Karnevskiy⁸⁵, S.N. Karpov⁶⁷, Z.M. Karpova⁶⁷, K. Karthik¹¹¹, V. Kartvelishvili⁷⁴, A.N. Karyukhin¹³¹, K. Kasahara¹⁶¹, L. Kashif¹⁷³, R.D. Kass¹¹², A. Kastanas¹⁵, Y. Kataoka¹⁵⁶, C. Kato¹⁵⁶, A. Katre⁵¹, J. Katzy⁴⁴, K. Kawagoe⁷², T. Kawamoto¹⁵⁶, G. Kawamura⁵⁶, S. Kazama¹⁵⁶, V.F. Kazanin^{110,3}, R. Keeler¹⁶⁹, R. Kehoe⁴², J.S. Keller⁴⁴, J.J. Kempster⁷⁹, K. Kentaro¹⁰⁴, H. Keoshkerian¹⁵⁹, O. Kepka¹²⁸, B.P. Kerševan⁷⁷, S. Kersten¹⁷⁵, R.A. Keyes⁸⁹, M. Khader¹⁶⁶, F. Khalil-zada¹², A. Khanov¹¹⁵, A.G. Kharlamov^{110,3}, T.J. Khoo⁵¹, V. Khovanskii⁹⁸, E. Khramov⁶⁷, J. Khubua^{53b,24}, S. Kido⁶⁹, H.Y. Kim⁸, S.H. Kim¹⁶¹, Y.K. Kim³³, N. Kimura¹⁵⁵, O.M. Kind¹⁷, B.T. King⁷⁶, M. King¹⁶⁷, S.B. King¹⁶⁸, J. Kirk¹³², A.E. Kiryunin¹⁰², T. Kishimoto⁶⁹, D. Kisiielewska^{40a}, F. Kiss⁵⁰, K. Kiuchi¹⁶¹, O. Kivernyk¹³⁷, E. Kladiva^{145b}, M.H. Klein³⁷, M. Klein⁷⁶, U. Klein⁷⁶, K. Kleinknecht⁸⁵, P. Klimek¹⁰⁹, A. Klimentov²⁷, R. Klingenberg⁴⁵, J.A. Klinger¹⁴⁰, T. Klioutchnikova³², E.-E. Kluge^{60a}, P. Kluit¹⁰⁸, S. Kluth¹⁰², J. Knapik⁴¹, E. Kneringer⁶⁴, E.B.F.G. Knoops⁸⁷, A. Knue⁵⁵, A. Kobayashi¹⁵⁶, D. Kobayashi¹⁵⁸, T. Kobayashi¹⁵⁶, M. Kobel⁴⁶, M. Kocian¹⁴⁴, P. Kodys¹³⁰, T. Koffas³¹, E. Koffeman¹⁰⁸, T. Koi¹⁴⁴, H. Kolanoski¹⁷, M. Kolb^{60b}, I. Koletsou⁵, A.A. Komar^{97,*}, Y. Komori¹⁵⁶, T. Kondo⁶⁸,

N. Kondrashova⁴⁴, K. Köneke⁵⁰, A.C. König¹⁰⁷, T. Kono^{68,25}, R. Konoplich^{111,26}, N. Konstantinidis⁸⁰, R. Kopeliansky⁶³, S. Koperny^{40a}, L. Köpke⁸⁵, A.K. Kopp⁵⁰, K. Korcyl⁴¹, K. Kordas¹⁵⁵, A. Korn⁸⁰, A.A. Korol^{110,3}, I. Korolkov¹³, E.V. Korolkova¹⁴⁰, O. Kortner¹⁰², S. Kortner¹⁰², T. Kosek¹³⁰, V.V. Kostyukhin²³, A. Kotwal⁴⁷, A. Kourkouveli-Charalampidi¹⁵⁵, C. Kourkouvelis⁹, V. Kouskoura²⁷, A.B. Kowalewska⁴¹, R. Kowalewski¹⁶⁹, T.Z. Kowalski^{40a}, C. Kozakai¹⁵⁶, W. Kozanecki¹³⁷, A.S. Kozhin¹³¹, V.A. Kramarenko¹⁰⁰, G. Kramberger⁷⁷, D. Krasnopevtsev⁹⁹, M.W. Krasny⁸², A. Krasznahorkay³², J.K. Kraus²³, A. Kravchenko²⁷, M. Kretz^{60c}, J. Kretzschmar⁷⁶, K. Kreutzfeldt⁵⁴, P. Krieger¹⁵⁹, K. Krizka³³, K. Kroeninger⁴⁵, H. Kroha¹⁰², J. Kroll¹²³, J. Kroseberg²³, J. Krstic¹⁴, U. Kruchonak⁶⁷, H. Krüger²³, N. Krumnack⁶⁶, A. Kruse¹⁷³, M.C. Kruse⁴⁷, M. Kruskal²⁴, T. Kubota⁹⁰, H. Kucuk⁸⁰, S. Kuday^{4b}, J.T. Kuechler¹⁷⁵, S. Kuehn⁵⁰, A. Kugel^{60c}, F. Kuger¹⁷⁴, A. Kuhl¹³⁸, T. Kuhl⁴⁴, V. Kukhtin⁶⁷, R. Kukla¹³⁷, Y. Kulchitsky⁹⁴, S. Kuleshov^{34b}, M. Kuna^{133a,133b}, T. Kunigo⁷⁰, A. Kupco¹²⁸, H. Kurashige⁶⁹, Y.A. Kurochkin⁹⁴, V. Kus¹²⁸, E.S. Kuwertz¹⁶⁹, M. Kuze¹⁵⁸, J. Kvita¹¹⁶, T. Kwan¹⁶⁹, D. Kyriazopoulos¹⁴⁰, A. La Rosa¹⁰², J.L. La Rosa Navarro^{26d}, L. La Rotonda^{39a,39b}, C. Lacasta¹⁶⁷, F. Lacava^{133a,133b}, J. Lacey³¹, H. Lacker¹⁷, D. Lacour⁸², V.R. Lacuesta¹⁶⁷, E. Ladygin⁶⁷, R. Lafaye⁵, B. Laforge⁸², T. Lagouri¹⁷⁶, S. Lai⁵⁶, S. Lammers⁶³, W. Lampl⁷, E. Lançon¹³⁷, U. Landgraf⁵⁰, M.P.J. Landon⁷⁸, V.S. Lang^{60a}, J.C. Lange¹³, A.J. Lankford¹⁶³, F. Lanni²⁷, K. Lantzsche²³, A. Lanza^{122a}, S. Laplace⁸², C. Lapoire³², J.F. Laporte¹³⁷, T. Lari^{93a}, F. Lasagni Manghi^{22a,22b}, M. Lassnig³², P. Laurelli⁴⁹, W. Lavrijsen¹⁶, A.T. Law¹³⁸, P. Laycock⁷⁶, T. Lazovich⁵⁹, M. Lazzaroni^{93a,93b}, B. Le⁹⁰, O. Le Dortz⁸², E. Le Guirriec⁸⁷, E.P. Le Quilleuc¹³⁷, M. LeBlanc¹⁶⁹, T. LeCompte⁶, F. Ledroit-Guillon⁵⁷, C.A. Lee²⁷, S.C. Lee¹⁵², L. Lee¹, G. Lefebvre⁸², M. Lefebvre¹⁶⁹, F. Legger¹⁰¹, C. Leggett¹⁶, A. Lehan⁷⁶, G. Lehmann Miotto³², X. Lei⁷, W.A. Leight³¹, A. Leisos^{155,27}, A.G. Leister¹⁷⁶, M.A.L. Leite^{26d}, R. Leitner¹³⁰, D. Lellouch¹⁷², B. Lemmer⁵⁶, K.J.C. Leney⁸⁰, T. Lenz²³, B. Lenzi³², R. Leone⁷, S. Leone^{125a,125b}, C. Leonidopoulos⁴⁸, S. Leontsinis¹⁰, G. Lerner¹⁵⁰, C. Leroy⁹⁶, A.A.J. Lesage¹³⁷, C.G. Lester³⁰, M. Levchenko¹²⁴, J. Levêque⁵, D. Levin⁹¹, L.J. Levinson¹⁷², M. Levy¹⁹, D. Lewis⁷⁸, A.M. Leyko²³, M. Leyton⁴³, B. Li^{35b,15}, H. Li¹⁴⁹, H.L. Li³³, L. Li⁴⁷, L. Li^{35e}, Q. Li^{35a}, S. Li⁴⁷, X. Li⁸⁶, Y. Li¹⁴², Z. Liang^{35a}, B. Liberti^{134a}, A. Liblong¹⁵⁹, P. Lichard³², K. Lie¹⁶⁶, J. Liebal²³, W. Liebig¹⁵, A. Limosani¹⁵¹, S.C. Lin^{152,28}, T.H. Lin⁸⁵, B.E. Lindquist¹⁴⁹, A.E. Lioni⁵¹, E. Lipeles¹²³, A. Lipniacka¹⁵, M. Lisovsky^{60b}, T.M. Liss¹⁶⁶, A. Lister¹⁶⁸, A.M. Litke¹³⁸, B. Liu^{152,29}, D. Liu¹⁵², H. Liu⁹¹, H. Liu²⁷, J. Liu⁸⁷, J.B. Liu^{35b}, K. Liu⁸⁷, L. Liu¹⁶⁶, M. Liu⁴⁷, M. Liu^{35b}, Y.L. Liu^{35b}, Y. Liu^{35b}, M. Livan^{122a,122b}, A. Lleres⁵⁷, J. Llorente Merino^{35a}, S.L. Lloyd⁷⁸, F. Lo Sterzo¹⁵², E. Lobodzinska⁴⁴, P. Loch⁷, W.S. Lockman¹³⁸, F.K. Loebinger⁸⁶, A.E. Loevschall-Jensen³⁸, K.M. Loew²⁵, A. Loginov^{176,*}, T. Lohse¹⁷, K. Lohwasser⁴⁴, M. Lokajicek¹²⁸, B.A. Long²⁴, J.D. Long¹⁶⁶, R.E. Long⁷⁴, L. Longo^{75a,75b}, K.A. Looper¹¹², L. Lopes^{127a}, D. Lopez Mateos⁵⁹, B. Lopez Paredes¹⁴⁰, I. Lopez Paz¹³, A. Lopez Solis⁸², J. Lorenz¹⁰¹, N. Lorenzo Martinez⁶³, M. Losada²¹, P.J. Lösel¹⁰¹, X. Lou^{35a}, A. Lounis¹¹⁸, J. Love⁶, P.A. Love⁷⁴, H. Lu^{62a}, N. Lu⁹¹, H.J. Lubatti¹³⁹, C. Luci^{133a,133b}, A. Lucotte⁵⁷, C. Luedtke⁵⁰, F. Luehring⁶³, W. Lukas⁶⁴, L. Luminari^{133a}, O. Lundberg^{147a,147b}, B. Lund-Jensen¹⁴⁸, P.M. Luzi⁸², D. Lynn²⁷, R. Lysak¹²⁸, E. Lytken⁸³, V. Lyubushkin⁶⁷, H. Ma²⁷, L.L. Ma^{35d}, Y. Ma^{35d}, G. Maccarrone⁴⁹, A. Macchiolo¹⁰², C.M. Macdonald¹⁴⁰, B. Maček⁷⁷, J. Machado Miguens^{123,127b}, D. Madaffari⁸⁷, R. Madar³⁶, H.J. Maddocks¹⁶⁵, W.F. Mader⁴⁶, A. Madsen⁴⁴, J. Maeda⁶⁹, S. Maeland¹⁵, T. Maeno²⁷, A. Maevskiy¹⁰⁰, E. Magradze⁵⁶, J. Mahlstedt¹⁰⁸, C. Maiani¹¹⁸, C. Maidantchik^{26a}, A.A. Maier¹⁰², T. Maier¹⁰¹, A. Maio^{127a,127b,127d}, S. Majewski¹¹⁷, Y. Makida⁶⁸, N. Makovec¹¹⁸, B. Malaescu⁸², Pa. Malecki⁴¹, V.P. Maleev¹²⁴, F. Malek⁵⁷, U. Mallik⁶⁵, D. Malon⁶, C. Malone¹⁴⁴, S. Maltezos¹⁰, S. Malyukov³², J. Mamuzic¹⁶⁷, G. Mancini⁴⁹, B. Mandelli³², L. Mandelli^{93a}, I. Mandić⁷⁷, J. Maneira^{127a,127b}, L. Manhaes de Andrade Filho^{26b}, J. Manjarres Ramos^{160b}, A. Mann¹⁰¹, A. Manousos³², B. Mansoulie¹³⁷, J.D. Mansour^{35a}, R. Mantifel⁸⁹, M. Mantoani⁵⁶, S. Manzoni^{93a,93b}, L. Mapelli³², G. Marceca²⁹, L. March⁵¹, G. Marchiori⁸², M. Marcisovsky¹²⁸, M. Marjanovic¹⁴, D.E. Marley⁹¹, F. Marroquim^{26a}, S.P. Marsden⁸⁶, Z. Marshall¹⁶, S. Marti-Garcia¹⁶⁷, B. Martin⁹², T.A. Martin¹⁷⁰, V.J. Martin⁴⁸, B. Martin dit Latour¹⁵, M. Martinez^{13,18}, V.I. Martinez Outschoorn¹⁶⁶, S. Martin-Haugh¹³², V.S. Martoiu^{28b}, A.C. Martyniuk⁸⁰, M. Marx¹³⁹, A. Marzin³², L. Masetti⁸⁵, T. Mashimo¹⁵⁶, R. Mashinistov⁹⁷, J. Masik⁸⁶, A.L. Maslennikov^{110,3}, I. Massa^{22a,22b}, L. Massa^{22a,22b}, P. Mastrandrea⁵, A. Mastroberardino^{39a,39b}, T. Masubuchi¹⁵⁶, P. Mättig¹⁷⁵, J. Mattmann⁸⁵, J. Maurer^{28b}, S.J. Maxfield⁷⁶, D.A. Maximov^{110,3}, R. Mazini¹⁵², S.M. Mazza^{93a,93b}, N.C. Mc Fadden¹⁰⁶, G. Mc Goldrick¹⁵⁹, S.P. Mc Kee⁹¹, A. McCarn⁹¹, R.L. McCarthy¹⁴⁹, T.G. McCarthy¹⁰², L.I. McClymont⁸⁰,

E.F. McDonald⁹⁰, K.W. McFarlane^{58,*}, J.A. McFayden⁸⁰, G. Mchedlidze⁵⁶, S.J. McMahon¹³², R.A. McPherson^{169,12}, M. Medinnis⁴⁴, S. Meehan¹³⁹, S. Mehlhase¹⁰¹, A. Mehta⁷⁶, K. Meier^{60a}, C. Meineck¹⁰¹, B. Meirose⁴³, D. Melini¹⁶⁷, B.R. Mellado Garcia^{146c}, M. Melo^{145a}, F. Meloni¹⁸, A. Mengarelli^{22a,22b}, S. Menke¹⁰², E. Meoni¹⁶², S. Mergelmeyer¹⁷, P. Mermod⁵¹, L. Merola^{105a,105b}, C. Meroni^{93a}, F.S. Merritt³³, A. Messina^{133a,133b}, J. Metcalfe⁶, A.S. Mete¹⁶³, C. Meyer⁸⁵, C. Meyer¹²³, J.-P. Meyer¹³⁷, J. Meyer¹⁰⁸, H. Meyer Zu Theenhausen^{60a}, F. Miano¹⁵⁰, R.P. Middleton¹³², S. Miglioranza^{52a,52b}, L. Mijović²³, G. Mikenberg¹⁷², M. Mikestikova¹²⁸, M. Mikuž⁷⁷, M. Milesi⁹⁰, A. Milic⁶⁴, D.W. Miller³³, C. Mills⁴⁸, A. Milov¹⁷², D.A. Milstead^{147a,147b}, A.A. Minaenko¹³¹, Y. Minami¹⁵⁶, I.A. Minashvili⁶⁷, A.I. Mincer¹¹¹, B. Mindur^{40a}, M. Mineev⁶⁷, Y. Ming¹⁷³, L.M. Mir¹³, K.P. Mistry¹²³, T. Mitani¹⁷¹, J. Mitrevski¹⁰¹, V.A. Mitsou¹⁶⁷, A. Miucci⁵¹, P.S. Miyagawa¹⁴⁰, J.U. Mjörnmark⁸³, T. Moa^{147a,147b}, K. Mochizuki⁹⁶, S. Mohapatra³⁷, S. Molander^{147a,147b}, R. Moles-Valls²³, R. Monden⁷⁰, M.C. Mondragon⁹², K. Mönig⁴⁴, J. Monk³⁸, E. Monnier⁸⁷, A. Montalbano¹⁴⁹, J. Montejo Berlingen³², F. Monticelli⁷³, S. Monzani^{93a,93b}, R.W. Moore³, N. Morange¹¹⁸, D. Moreno²¹, M. Moreno Llacer⁵⁶, P. Morettini^{52a}, D. Mori¹⁴³, T. Mori¹⁵⁶, M. Morii⁵⁹, M. Morinaga¹⁵⁶, V. Morisbak¹²⁰, S. Moritz⁸⁵, A.K. Morley¹⁵¹, G. Mornacchi³², J.D. Morris⁷⁸, S.S. Mortensen³⁸, L. Morvaj¹⁴⁹, M. Mosidze^{53b}, J. Moss¹⁴⁴, K. Motohashi¹⁵⁸, R. Mount¹⁴⁴, E. Mountricha²⁷, S.V. Mouraviev^{97,*}, E.J.W. Moyse⁸⁸, S. Muanza⁸⁷, R.D. Mudd¹⁹, F. Mueller¹⁰², J. Mueller¹²⁶, R.S.P. Mueller¹⁰¹, T. Mueller³⁰, D. Muenstermann⁷⁴, P. Mullen⁵⁵, G.A. Mullier¹⁸, F.J. Munoz Sanchez⁸⁶, J.A. Murillo Quijada¹⁹, W.J. Murray^{170,132}, H. Musheghyan⁵⁶, M. Muškinja⁷⁷, A.G. Myagkov^{131,30}, M. Myska¹²⁹, B.P. Nachman¹⁴⁴, O. Nackenhorst⁵¹, K. Nagai¹²¹, R. Nagai^{68,25}, K. Nagano⁶⁸, Y. Nagasaka⁶¹, K. Nagata¹⁶¹, M. Nagel⁵⁰, E. Nagy⁸⁷, A.M. Nairz³², Y. Nakahama³², K. Nakamura⁶⁸, T. Nakamura¹⁵⁶, I. Nakano¹¹³, H. Namasivayam⁴³, R.F. Naranjo Garcia⁴⁴, R. Narayan¹¹, D.I. Narrias Villar^{60a}, I. Naryshkin¹²⁴, T. Naumann⁴⁴, G. Navarro²¹, R. Nayyar⁷, H.A. Neal⁹¹, P.Yu. Nechaeva⁹⁷, T.J. Neep⁸⁶, P.D. Nef¹⁴⁴, A. Negri^{122a,122b}, M. Negrini^{22a}, S. Nektarijevic¹⁰⁷, C. Nellist¹¹⁸, A. Nelson¹⁶³, S. Nemecek¹²⁸, P. Nemethy¹¹¹, A.A. Nepomuceno^{26a}, M. Nessi^{32,31}, M.S. Neubauer¹⁶⁶, M. Neumann¹⁷⁵, R.M. Neves¹¹¹, P. Nevski²⁷, P.R. Newman¹⁹, D.H. Nguyen⁶, T. Nguyen Manh⁹⁶, R.B. Nickerson¹²¹, R. Nicolaidou¹³⁷, J. Nielsen¹³⁸, A. Nikiforov¹⁷, V. Nikolaenko^{131,30}, I. Nikolic-Audit⁸², K. Nikolopoulos¹⁹, J.K. Nilsen¹²⁰, P. Nilsson²⁷, Y. Ninomiya¹⁵⁶, A. Nisati^{133a}, R. Nisius¹⁰², T. Nobe¹⁵⁶, L. Nodulman⁶, M. Nomachi¹¹⁹, I. Nomidis³¹, T. Nooney⁷⁸, S. Norberg¹¹⁴, M. Nordberg³², N. Norjoharuddeen¹²¹, O. Novgorodova⁴⁶, S. Nowak¹⁰², M. Nozaki⁶⁸, L. Nozka¹¹⁶, K. Ntekas¹⁰, E. Nurse⁸⁰, F. Nuti⁹⁰, F. O'grady⁷, D.C. O'Neil¹⁴³, A.A. O'Rourke⁴⁴, V. O'Shea⁵⁵, F.G. Oakham^{31,4}, H. Oberlack¹⁰², T. Obermann²³, J. Ocariz⁸², A. Ochi⁶⁹, I. Ochoa³⁷, J.P. Ochoa-Ricoux^{34a}, S. Oda⁷², S. Odaka⁶⁸, H. Ogren⁶³, A. Oh⁸⁶, S.H. Oh⁴⁷, C.C. Ohm¹⁶, H. Ohman¹⁶⁵, H. Oide³², H. Okawa¹⁶¹, Y. Okumura³³, T. Okuyama⁶⁸, A. Olariu^{28b}, L.F. Oleiro Seabra^{127a}, S.A. Olivares Pino⁴⁸, D. Oliveira Damazio²⁷, A. Olszewski⁴¹, J. Olszowska⁴¹, A. Onofre^{127a,127e}, K. Onogi¹⁰⁴, P.U.E. Onyisi^{11,22}, M.J. Oreglia³³, Y. Oren¹⁵⁴, D. Orestano^{135a,135b}, N. Orlando^{62b}, R.S. Orr¹⁵⁹, B. Osculati^{52a,52b}, R. Ospanov⁸⁶, G. Otero y Garzon²⁹, H. Otono⁷², M. Ouchrif^{136d}, F. Ould-Saada¹²⁰, A. Ouraou¹³⁷, K.P. Oussoren¹⁰⁸, Q. Ouyang^{35a}, M. Owen⁵⁵, R.E. Owen¹⁹, V.E. Ozcan^{20a}, N. Ozturk⁸, K. Pachal¹⁴³, A. Pacheco Pages¹³, L. Pacheco Rodriguez¹³⁷, C. Padilla Aranda¹³, M. Pagáčová⁵⁰, S. Pagan Griso¹⁶, F. Paige²⁷, P. Pais⁸⁸, K. Pajchel¹²⁰, G. Palacino^{160b}, S. Palazzo^{39a,39b}, S. Palestini³², M. Palka^{40b}, D. Pallin³⁶, A. Palma^{127a,127b}, E.St. Panagiotopoulou¹⁰, C.E. Pandini⁸², J.G. Panduro Vazquez⁷⁹, P. Pani^{147a,147b}, S. Panitkin²⁷, D. Pantea^{28b}, L. Paolozzi⁵¹, Th.D. Papadopoulou¹⁰, K. Papageorgiou¹⁵⁵, A. Paramonov⁶, D. Paredes Hernandez¹⁷⁶, A.J. Parker⁷⁴, M.A. Parker³⁰, K.A. Parker¹⁴⁰, F. Parodi^{52a,52b}, J.A. Parsons³⁷, U. Parzefall⁵⁰, V.R. Pascuzzi¹⁵⁹, E. Pasqualucci^{133a}, S. Passaggio^{52a}, Fr. Pastore⁷⁹, G. Pásztor^{31,32}, S. Pataraja¹⁷⁵, J.R. Pater⁸⁶, T. Pauly³², J. Pearce¹⁶⁹, B. Pearson¹¹⁴, L.E. Pedersen³⁸, M. Pedersen¹²⁰, S. Pedraza Lopez¹⁶⁷, R. Pedro^{127a,127b}, S.V. Peleganchuk^{110,3}, D. Pelikan¹⁶⁵, O. Penc¹²⁸, C. Peng^{35a}, H. Peng^{35b}, J. Penwell⁶³, B.S. Peralva^{26b}, M.M. Perego¹³⁷, D.V. Perepelitsa²⁷, E. Perez Codina^{160a}, L. Perini^{93a,93b}, H. Pernegger³², S. Perrella^{105a,105b}, R. Peschke⁴⁴, V.D. Peshekhonov⁶⁷, K. Peters⁴⁴, R.F.Y. Peters⁸⁶, B.A. Petersen³², T.C. Petersen³⁸, E. Petit⁵⁷, A. Petridis¹, C. Petridou¹⁵⁵, P. Petroff¹¹⁸, E. Petrolo^{133a}, M. Petrov¹²¹, F. Petrucci^{135a,135b}, N.E. Pettersson⁸⁸, A. Peyaud¹³⁷, R. Pezoa^{34b}, P.W. Phillips¹³², G. Piacquadio^{144,33}, E. Pianori¹⁷⁰, A. Picazio⁸⁸, E. Piccaro⁷⁸, M. Piccinini^{22a,22b}, M.A. Pickering¹²¹, R. Piegaia²⁹, J.E. Pilcher³³, A.D. Pilkington⁸⁶, A.W.J. Pin⁸⁶,

M. Pinamonti ^{164a,164c,34}, J.L. Pinfold ³, A. Pingel ³⁸, S. Pires ⁸², H. Pirumov ⁴⁴, M. Pitt ¹⁷², L. Plazak ^{145a}, M.-A. Pleier ²⁷, V. Pleskot ⁸⁵, E. Plotnikova ⁶⁷, P. Plucinski ⁹², D. Pluth ⁶⁶, R. Poettgen ^{147a,147b}, L. Poggioli ¹¹⁸, D. Pohl ²³, G. Polesello ^{122a}, A. Poley ⁴⁴, A. Policicchio ^{39a,39b}, R. Polifka ¹⁵⁹, A. Polini ^{22a}, C.S. Pollard ⁵⁵, V. Polychronakos ²⁷, K. Pommès ³², L. Pontecorvo ^{133a}, B.G. Pope ⁹², G.A. Popeneciu ^{28c}, D.S. Popovic ¹⁴, A. Poppleton ³², S. Pospisil ¹²⁹, K. Potamianos ¹⁶, I.N. Potrap ⁶⁷, C.J. Potter ³⁰, C.T. Potter ¹¹⁷, G. Poulard ³², J. Poveda ³², V. Pozdnyakov ⁶⁷, M.E. Pozo Astigarraga ³², P. Pralavorio ⁸⁷, A. Pranko ¹⁶, S. Prell ⁶⁶, D. Price ⁸⁶, L.E. Price ⁶, M. Primavera ^{75a}, S. Prince ⁸⁹, M. Proissl ⁴⁸, K. Prokofiev ^{62c}, F. Prokoshin ^{34b}, S. Protopopescu ²⁷, J. Proudfoot ⁶, M. Przybycien ^{40a}, D. Puddu ^{135a,135b}, M. Purohit ^{27,35}, P. Puzo ¹¹⁸, J. Qian ⁹¹, G. Qin ⁵⁵, Y. Qin ⁸⁶, A. Quadt ⁵⁶, W.B. Quayle ^{164a,164b}, M. Queitsch-Maitland ⁸⁶, D. Quilty ⁵⁵, S. Raddum ¹²⁰, V. Radeka ²⁷, V. Radescu ^{60b}, S.K. Radhakrishnan ¹⁴⁹, P. Radloff ¹¹⁷, P. Rados ⁹⁰, F. Ragusa ^{93a,93b}, G. Rahal ¹⁷⁸, J.A. Raine ⁸⁶, S. Rajagopalan ²⁷, M. Rammensee ³², C. Rangel-Smith ¹⁶⁵, M.G. Ratti ^{93a,93b}, F. Rauscher ¹⁰¹, S. Rave ⁸⁵, T. Ravenscroft ⁵⁵, I. Ravinovich ¹⁷², M. Raymond ³², A.L. Read ¹²⁰, N.P. Readioff ⁷⁶, M. Reale ^{75a,75b}, D.M. Rebuzzi ^{122a,122b}, A. Redelbach ¹⁷⁴, G. Redlinger ²⁷, R. Reece ¹³⁸, K. Reeves ⁴³, L. Rehnisch ¹⁷, J. Reichert ¹²³, H. Reisin ²⁹, C. Rembser ³², H. Ren ^{35a}, M. Rescigno ^{133a}, S. Resconi ^{93a}, O.L. Rezanova ^{110,3}, P. Reznicek ¹³⁰, R. Rezvani ⁹⁶, R. Richter ¹⁰², S. Richter ⁸⁰, E. Richter-Was ^{40b}, O. Ricken ²³, M. Ridel ⁸², P. Rieck ¹⁷, C.J. Riegel ¹⁷⁵, J. Rieger ⁵⁶, O. Rifki ¹¹⁴, M. Rijssenbeek ¹⁴⁹, A. Rimoldi ^{122a,122b}, M. Rimoldi ¹⁸, L. Rinaldi ^{22a}, B. Ristić ⁵¹, E. Ritsch ³², I. Riu ¹³, F. Rizatdinova ¹¹⁵, E. Rizvi ⁷⁸, C. Rizzi ¹³, S.H. Robertson ^{89,12}, A. Robichaud-Veronneau ⁸⁹, D. Robinson ³⁰, J.E.M. Robinson ⁴⁴, A. Robson ⁵⁵, C. Roda ^{125a,125b}, Y. Rodina ⁸⁷, A. Rodriguez Perez ¹³, D. Rodriguez Rodriguez ¹⁶⁷, S. Roe ³², C.S. Rogan ⁵⁹, O. Røhne ¹²⁰, A. Romaniouk ⁹⁹, M. Romano ^{22a,22b}, S.M. Romano Saez ³⁶, E. Romero Adam ¹⁶⁷, N. Rompotis ¹³⁹, M. Ronzani ⁵⁰, L. Roos ⁸², E. Ros ¹⁶⁷, S. Rosati ^{133a}, K. Rosbach ⁵⁰, P. Rose ¹³⁸, O. Rosenthal ¹⁴², N.-A. Rosien ⁵⁶, V. Rossetti ^{147a,147b}, E. Rossi ^{105a,105b}, L.P. Rossi ^{52a}, J.H.N. Rosten ³⁰, R. Rosten ¹³⁹, M. Rotaru ^{28b}, I. Roth ¹⁷², J. Rothberg ¹³⁹, D. Rousseau ¹¹⁸, C.R. Royon ¹³⁷, A. Rozanov ⁸⁷, Y. Rozen ¹⁵³, X. Ruan ^{146c}, F. Rubbo ¹⁴⁴, M.S. Rudolph ¹⁵⁹, F. Rühr ⁵⁰, A. Ruiz-Martinez ³¹, Z. Rurikova ⁵⁰, N.A. Rusakovich ⁶⁷, A. Ruschke ¹⁰¹, H.L. Russell ¹³⁹, J.P. Rutherford ⁷, N. Ruthmann ³², Y.F. Ryabov ¹²⁴, M. Rybar ¹⁶⁶, G. Rybkin ¹¹⁸, S. Ryu ⁶, A. Ryzhov ¹³¹, G.F. Rzehorz ⁵⁶, A.F. Saavedra ¹⁵¹, G. Sabato ¹⁰⁸, S. Sacerdoti ²⁹, H.F.-W. Sadrozinski ¹³⁸, R. Sadykov ⁶⁷, F. Safai Tehrani ^{133a}, P. Saha ¹⁰⁹, M. Sahinsoy ^{60a}, M. Saimpert ¹³⁷, T. Saito ¹⁵⁶, H. Sakamoto ¹⁵⁶, Y. Sakurai ¹⁷¹, G. Salamanna ^{135a,135b}, A. Salamon ^{134a,134b}, J.E. Salazar Loyola ^{34b}, D. Salek ¹⁰⁸, P.H. Sales De Bruin ¹³⁹, D. Salihagic ¹⁰², A. Salnikov ¹⁴⁴, J. Salt ¹⁶⁷, D. Salvatore ^{39a,39b}, F. Salvatore ¹⁵⁰, A. Salvucci ^{62a}, A. Salzburger ³², D. Sammel ⁵⁰, D. Sampsonidis ¹⁵⁵, A. Sanchez ^{105a,105b}, J. Sánchez ¹⁶⁷, V. Sanchez Martinez ¹⁶⁷, H. Sandaker ¹²⁰, R.L. Sandbach ⁷⁸, H.G. Sander ⁸⁵, M. Sandhoff ¹⁷⁵, C. Sandoval ²¹, R. Sandstroem ¹⁰², D.P.C. Sankey ¹³², M. Sannino ^{52a,52b}, A. Sansoni ⁴⁹, C. Santoni ³⁶, R. Santonico ^{134a,134b}, H. Santos ^{127a}, I. Santoyo Castillo ¹⁵⁰, K. Sapp ¹²⁶, A. Saprionov ⁶⁷, J.G. Saraiva ^{127a,127d}, B. Sarrazin ²³, O. Sasaki ⁶⁸, Y. Sasaki ¹⁵⁶, K. Sato ¹⁶¹, G. Sauvage ^{5,*}, E. Sauvan ⁵, G. Savage ⁷⁹, P. Savard ^{159,4}, C. Sawyer ¹³², L. Sawyer ^{81,17}, J. Saxon ³³, C. Sbarra ^{22a}, A. Sbrizzi ^{22a,22b}, T. Scanlon ⁸⁰, D.A. Scannicchio ¹⁶³, M. Scarcella ¹⁵¹, V. Scarfone ^{39a,39b}, J. Schaarschmidt ¹⁷², P. Schacht ¹⁰², B.M. Schachtner ¹⁰¹, D. Schaefer ³², R. Schaefer ⁴⁴, J. Schaeffer ⁸⁵, S. Schaepe ²³, S. Schaetzel ^{60b}, U. Schäfer ⁸⁵, A.C. Schaffer ¹¹⁸, D. Schaile ¹⁰¹, R.D. Schamberger ¹⁴⁹, V. Scharf ^{60a}, V.A. Schegelsky ¹²⁴, D. Scheirich ¹³⁰, M. Schernau ¹⁶³, C. Schiavi ^{52a,52b}, S. Schier ¹³⁸, C. Schillo ⁵⁰, M. Schioppa ^{39a,39b}, S. Schlenker ³², K.R. Schmidt-Sommerfeld ¹⁰², K. Schmieden ³², C. Schmitt ⁸⁵, S. Schmitt ⁴⁴, S. Schmitz ⁸⁵, B. Schneider ^{160a}, U. Schnoor ⁵⁰, L. Schoeffel ¹³⁷, A. Schoening ^{60b}, B.D. Schoenrock ⁹², E. Schopf ²³, M. Schott ⁸⁵, J. Schovancova ⁸, S. Schramm ⁵¹, M. Schreyer ¹⁷⁴, N. Schuh ⁸⁵, M.J. Schultens ²³, H.-C. Schultz-Coulon ^{60a}, H. Schulz ¹⁷, M. Schumacher ⁵⁰, B.A. Schumm ¹³⁸, Ph. Schune ¹³⁷, A. Schwartzman ¹⁴⁴, T.A. Schwarz ⁹¹, Ph. Schwegler ¹⁰², H. Schweiger ⁸⁶, Ph. Schwemling ¹³⁷, R. Schwienhorst ⁹², J. Schwindling ¹³⁷, T. Schwindt ²³, G. Sciolla ²⁵, F. Scuri ^{125a,125b}, F. Scutti ⁹⁰, J. Searcy ⁹¹, P. Seema ²³, S.C. Seidel ¹⁰⁶, A. Seiden ¹³⁸, F. Seifert ¹²⁹, J.M. Seixas ^{26a}, G. Sekhniaidze ^{105a}, K. Sekhon ⁹¹, S.J. Sekula ⁴², D.M. Seliverstov ^{124,*}, N. Semprini-Cesari ^{22a,22b}, C. Serfon ¹²⁰, L. Serin ¹¹⁸, L. Serkin ^{164a,164b}, M. Sessa ^{135a,135b}, R. Seuster ¹⁶⁹, H. Severini ¹¹⁴, T. Sfiligoi ⁷⁷, F. Sforza ³², A. Sfyrla ⁵¹, E. Shabalina ⁵⁶, N.W. Shaikh ^{147a,147b}, L.Y. Shan ^{35a}, R. Shang ¹⁶⁶, J.T. Shank ²⁴, M. Shapiro ¹⁶, P.B. Shatalov ⁹⁸, K. Shaw ^{164a,164b}, S.M. Shaw ⁸⁶, A. Shcherbakova ^{147a,147b}, C.Y. Shehu ¹⁵⁰, P. Sherwood ⁸⁰, L. Shi ^{152,36}, S. Shimizu ⁶⁹, C.O. Shimmin ¹⁶³, M. Shimojima ¹⁰³, M. Shiyakova ^{67,37},

A. Shmeleva⁹⁷, D. Shoaleh Saadi⁹⁶, M.J. Shochet³³, S. Shojaii^{93a,93b}, S. Shrestha¹¹², E. Shulga⁹⁹, M.A. Shupe⁷, P. Sicho¹²⁸, A.M. Sickles¹⁶⁶, P.E. Sidebo¹⁴⁸, O. Sidiropoulou¹⁷⁴, D. Sidorov¹¹⁵, A. Sidoti^{22a,22b}, F. Siegert⁴⁶, Dj. Sijacki¹⁴, J. Silva^{127a,127d}, S.B. Silverstein^{147a}, V. Simak¹²⁹, O. Simard⁵, Lj. Simic¹⁴, S. Simion¹¹⁸, E. Simioni⁸⁵, B. Simmons⁸⁰, D. Simon³⁶, M. Simon⁸⁵, P. Sinervo¹⁵⁹, N.B. Sinev¹¹⁷, M. Sioli^{22a,22b}, G. Siragusa¹⁷⁴, S.Yu. Sivoklov¹⁰⁰, J. Sjölin^{147a,147b}, M.B. Skinner⁷⁴, H.P. Skottowe⁵⁹, P. Skubic¹¹⁴, M. Slater¹⁹, T. Slavicek¹²⁹, M. Slawinska¹⁰⁸, K. Sliwa¹⁶², R. Slovak¹³⁰, V. Smakhtin¹⁷², B.H. Smart⁵, L. Smestad¹⁵, J. Smiesko^{145a}, S.Yu. Smirnov⁹⁹, Y. Smirnov⁹⁹, L.N. Smirnova^{100,38}, O. Smirnova⁸³, M.N.K. Smith³⁷, R.W. Smith³⁷, M. Smizanska⁷⁴, K. Smolek¹²⁹, A.A. Snesarev⁹⁷, S. Snyder²⁷, R. Sobie^{169,12}, F. Socher⁴⁶, A. Soffer¹⁵⁴, D.A. Soh¹⁵², G. Sokhrannyi⁷⁷, C.A. Solans Sanchez³², M. Solar¹²⁹, E.Yu. Soldatov⁹⁹, U. Soldevila¹⁶⁷, A.A. Solodkov¹³¹, A. Soloshenko⁶⁷, O.V. Solovyanov¹³¹, V. Solovye¹²⁴, P. Sommer⁵⁰, H. Son¹⁶², H.Y. Song^{35b,39}, A. Sood¹⁶, A. Sopczak¹²⁹, V. Sopko¹²⁹, V. Sorin¹³, D. Sosa^{60b}, C.L. Sotiropoulou^{125a,125b}, R. Soualah^{164a,164c}, A.M. Soukharev^{110,3}, D. South⁴⁴, B.C. Sowden⁷⁹, S. Spagnolo^{75a,75b}, M. Spalla^{125a,125b}, M. Spangenberg¹⁷⁰, F. Spanò⁷⁹, D. Sperlich¹⁷, F. Spettel¹⁰², R. Spighi^{22a}, G. Spigo³², L.A. Spiller⁹⁰, M. Spousta¹³⁰, R.D. St. Denis^{55,*}, A. Stabile^{93a}, R. Stamen^{60a}, S. Stamm¹⁷, E. Stanecka⁴¹, R.W. Stanek⁶, C. Stanescu^{135a}, M. Stanescu-Bellu⁴⁴, M.M. Stanitzki⁴⁴, S. Stapnes¹²⁰, E.A. Starchenko¹³¹, G.H. Stark³³, J. Stark⁵⁷, P. Staroba¹²⁸, P. Starovoitov^{60a}, S. Stärz³², R. Staszewski⁴¹, P. Steinberg²⁷, B. Stelzer¹⁴³, H.J. Stelzer³², O. Stelzer-Chilton^{160a}, H. Stenzel⁵⁴, G.A. Stewart⁵⁵, J.A. Stillings²³, M.C. Stockton⁸⁹, M. Stoebe⁸⁹, G. Stoicea^{28b}, P. Stolte⁵⁶, S. Stonjek¹⁰², A.R. Stradling⁸, A. Straessner⁴⁶, M.E. Stramaglia¹⁸, J. Strandberg¹⁴⁸, S. Strandberg^{147a,147b}, A. Strandlie¹²⁰, M. Strauss¹¹⁴, P. Strizenec^{145b}, R. Ströhmer¹⁷⁴, D.M. Strom¹¹⁷, R. Stroynowski⁴², A. Strubig¹⁰⁷, S.A. Stucci¹⁸, B. Stugu¹⁵, N.A. Styles⁴⁴, D. Su¹⁴⁴, J. Su¹²⁶, R. Subramaniam⁸¹, S. Suchek^{60a}, Y. Sugaya¹¹⁹, M. Suk¹²⁹, V.V. Sulin⁹⁷, S. Sultansoy^{4c}, T. Sumida⁷⁰, S. Sun⁵⁹, X. Sun^{35a}, J.E. Sundermann⁵⁰, K. Suruliz¹⁵⁰, G. Susinno^{39a,39b}, M.R. Sutton¹⁵⁰, S. Suzuki⁶⁸, M. Svatos¹²⁸, M. Swiatkowski³³, I. Sykora^{145a}, T. Sykora¹³⁰, D. Ta⁵⁰, C. Taccini^{135a,135b}, K. Tackmann⁴⁴, J. Taenzer¹⁵⁹, A. Taffard¹⁶³, R. Tafirout^{160a}, N. Taiblum¹⁵⁴, H. Takai²⁷, R. Takashima⁷¹, T. Takeshita¹⁴¹, Y. Takubo⁶⁸, M. Talby⁸⁷, A.A. Talyshev^{110,3}, K.G. Tan⁹⁰, J. Tanaka¹⁵⁶, R. Tanaka¹¹⁸, S. Tanaka⁶⁸, B.B. Tannenwald¹¹², S. Tapia Araya^{34b}, S. Tapprogge⁸⁵, S. Tarem¹⁵³, G.F. Tartarelli^{93a}, P. Tas¹³⁰, M. Tasevsky¹²⁸, T. Tashiro⁷⁰, E. Tassi^{39a,39b}, A. Tavares Delgado^{127a,127b}, Y. Tayalati^{136d}, A.C. Taylor¹⁰⁶, G.N. Taylor⁹⁰, P.T.E. Taylor⁹⁰, W. Taylor^{160b}, F.A. Teischinger³², P. Teixeira-Dias⁷⁹, K.K. Temming⁵⁰, D. Temple¹⁴³, H. Ten Kate³², P.K. Teng¹⁵², J.J. Teoh¹¹⁹, F. Tepel¹⁷⁵, S. Terada⁶⁸, K. Terashi¹⁵⁶, J. Terron⁸⁴, S. Terzo¹⁰², M. Testa⁴⁹, R.J. Teuscher^{159,12}, T. Theveneaux-Pelzer⁸⁷, J.P. Thomas¹⁹, J. Thomas-Wilsker⁷⁹, E.N. Thompson³⁷, P.D. Thompson¹⁹, A.S. Thompson⁵⁵, L.A. Thomsen¹⁷⁶, E. Thomson¹²³, M. Thomson³⁰, M.J. Tibbetts¹⁶, R.E. Ticse Torres⁸⁷, V.O. Tikhomirov^{97,40}, Yu.A. Tikhonov^{110,3}, S. Timoshenko⁹⁹, P. Tipton¹⁷⁶, S. Tisserant⁸⁷, K. Todome¹⁵⁸, T. Todorov^{5,*}, S. Todorova-Nova¹³⁰, J. Tojo⁷², S. Tokár^{145a}, K. Tokushuku⁶⁸, E. Tolley⁵⁹, L. Tomlinson⁸⁶, M. Tomoto¹⁰⁴, L. Tompkins^{144,41}, K. Toms¹⁰⁶, B. Tong⁵⁹, E. Torrence¹¹⁷, H. Torres¹⁴³, E. Torró Pastor¹³⁹, J. Toth^{87,42}, F. Touchard⁸⁷, D.R. Tovey¹⁴⁰, T. Trefzger¹⁷⁴, A. Tricoli²⁷, I.M. Trigger^{160a}, S. Trincas-Duvoid⁸², M.F. Tripiana¹³, W. Trischuk¹⁵⁹, B. Trocmé⁵⁷, A. Trofymov⁴⁴, C. Troncon^{93a}, M. Trottier-McDonald¹⁶, M. Trovatelli¹⁶⁹, L. Truong^{164a,164c}, M. Trzebinski⁴¹, A. Trzupek⁴¹, J.C.-L. Tseng¹²¹, P.V. Tsiarehsha⁹⁴, G. Tsipolitis¹⁰, N. Tsirintanis⁹, S. Tsiskaridze¹³, V. Tsiskaridze⁵⁰, E.G. Tskhadadze^{53a}, K.M. Tsui^{62a}, I.I. Tsukerman⁹⁸, V. Tsulaia¹⁶, S. Tsuno⁶⁸, D. Tsybychev¹⁴⁹, A. Tudorache^{28b}, V. Tudorache^{28b}, A.N. Tuna⁵⁹, S.A. Tupputi^{22a,22b}, S. Turchikhin^{100,38}, D. Turecek¹²⁹, D. Turgeman¹⁷², R. Turra^{93a,93b}, A.J. Turvey⁴², P.M. Tuts³⁷, M. Tyndel¹³², G. Ucchielli^{22a,22b}, I. Ueda¹⁵⁶, M. Ughetto^{147a,147b}, F. Ukegawa¹⁶¹, G. Unal³², A. Undrus²⁷, G. Unel¹⁶³, F.C. Ungaro⁹⁰, Y. Unno⁶⁸, C. Unverdorben¹⁰¹, J. Urban^{145b}, P. Urquijo⁹⁰, P. Urrejola⁸⁵, G. Usai⁸, A. Usanova⁶⁴, L. Vacavant⁸⁷, V. Vacek¹²⁹, B. Vachon⁸⁹, C. Valderanis¹⁰¹, E. Valdes Santurio^{147a,147b}, N. Valencic¹⁰⁸, S. Valentini^{22a,22b}, A. Valero¹⁶⁷, L. Valery¹³, S. Valkar¹³⁰, S. Vallecorsa⁵¹, J.A. Valls Ferrer¹⁶⁷, W. Van Den Wollenberg¹⁰⁸, P.C. Van Der Deijl¹⁰⁸, R. van der Geer¹⁰⁸, H. van der Graaf¹⁰⁸, N. van Eldik¹⁵³, P. van Gemmeren⁶, J. Van Nieuwkoop¹⁴³, I. van Vulpen¹⁰⁸, M.C. van Woerden³², M. Vanadia^{133a,133b}, W. Vandelli³², R. Vanguri¹²³, A. Vaniachine¹³¹, P. Vankov¹⁰⁸, G. Vardanyan¹⁷⁷, R. Vari^{133a}, E.W. Varnes⁷, T. Varol⁴², D. Varouchas⁸², A. Vartapetian⁸, K.E. Varvell¹⁵¹, J.G. Vasquez¹⁷⁶, F. Vazeille³⁶, T. Vazquez Schroeder⁸⁹, J. Veatch⁵⁶, L.M. Veloce¹⁵⁹, F. Veloso^{127a,127c}, S. Veneziano^{133a},

A. Ventura^{75a,75b}, M. Venturi¹⁶⁹, N. Venturi¹⁵⁹, A. Venturini²⁵, V. Vercesi^{122a}, M. Verducci^{133a,133b}, W. Verkerke¹⁰⁸, J.C. Vermeulen¹⁰⁸, A. Vest^{46,43}, M.C. Vetterli^{143,4}, O. Viazlo⁸³, I. Vichou^{166,*}, T. Vickey¹⁴⁰, O.E. Vickey Boeriu¹⁴⁰, G.H.A. Viehhauser¹²¹, S. Viel¹⁶, L. Vignani¹²¹, R. Vigne⁶⁴, M. Villa^{22a,22b}, M. Villaplana Perez^{93a,93b}, E. Vilucchi⁴⁹, M.G. Vincker³¹, V.B. Vinogradov⁶⁷, C. Vittori^{22a,22b}, I. Vivarelli¹⁵⁰, S. Vlachos¹⁰, M. Vlasak¹²⁹, M. Vogel¹⁷⁵, P. Vokac¹²⁹, G. Volpi^{125a,125b}, M. Volpi⁹⁰, H. von der Schmitt¹⁰², E. von Toerne²³, V. Vorobel¹³⁰, K. Vorobev⁹⁹, M. Vos¹⁶⁷, R. Voss³², J.H. Vossebeld⁷⁶, N. Vranjes¹⁴, M. Vranjes Milosavljevic¹⁴, V. Vrba¹²⁸, M. Vreeswijk¹⁰⁸, R. Vuillermet³², I. Vukotic³³, Z. Vykydal¹²⁹, P. Wagner²³, W. Wagner¹⁷⁵, H. Wahlberg⁷³, S. Wahrmund⁴⁶, J. Wakabayashi¹⁰⁴, J. Walder⁷⁴, R. Walker¹⁰¹, W. Walkowiak¹⁴², V. Wallangen^{147a,147b}, C. Wang^{35c}, C. Wang^{35d,87}, F. Wang¹⁷³, H. Wang¹⁶, H. Wang⁴², J. Wang⁴⁴, J. Wang¹⁵¹, K. Wang⁸⁹, R. Wang⁶, S.M. Wang¹⁵², T. Wang²³, T. Wang³⁷, W. Wang^{35b}, X. Wang¹⁷⁶, C. Wanotayaroj¹¹⁷, A. Warburton⁸⁹, C.P. Ward³⁰, D.R. Wardrope⁸⁰, A. Washbrook⁴⁸, P.M. Watkins¹⁹, A.T. Watson¹⁹, M.F. Watson¹⁹, G. Watts¹³⁹, S. Watts⁸⁶, B.M. Waugh⁸⁰, S. Webb⁸⁵, M.S. Weber¹⁸, S.W. Weber¹⁷⁴, J.S. Webster⁶, A.R. Weidberg¹²¹, B. Weinert⁶³, J. Weingarten⁵⁶, C. Weiser⁵⁰, H. Weits¹⁰⁸, P.S. Wells³², T. Wenaus²⁷, T. Wengler³², S. Wenig³², N. Wermes²³, M. Werner⁵⁰, M.D. Werner⁶⁶, P. Werner³², M. Wessels^{60a}, J. Wetter¹⁶², K. Whalen¹¹⁷, N.L. Whallon¹³⁹, A.M. Wharton⁷⁴, A. White⁸, M.J. White¹, R. White^{34b}, D. Whiteson¹⁶³, F.J. Wickens¹³², W. Wiedenmann¹⁷³, M. Wielers¹³², P. Wienemann²³, C. Wiglesworth³⁸, L.A.M. Wiik-Fuchs²³, A. Wildauer¹⁰², F. Wilk⁸⁶, H.G. Wilkens³², H.H. Williams¹²³, S. Williams¹⁰⁸, C. Willis⁹², S. Willocq⁸⁸, J.A. Wilson¹⁹, I. Wingerter-Seez⁵, F. Winklmeier¹¹⁷, O.J. Winston¹⁵⁰, B.T. Winter²³, M. Wittgen¹⁴⁴, J. Wittkowski¹⁰¹, M.W. Wolter⁴¹, H. Wolters^{127a,127c}, S.D. Worm¹³², B.K. Wosiek⁴¹, J. Wotschack³², M.J. Woudstra⁸⁶, K.W. Wozniak⁴¹, M. Wu⁵⁷, M. Wu³³, S.L. Wu¹⁷³, X. Wu⁵¹, Y. Wu⁹¹, T.R. Wyatt⁸⁶, B.M. Wynne⁴⁸, S. Xella³⁸, D. Xu^{35a}, L. Xu²⁷, B. Yabsley¹⁵¹, S. Yacoob^{146a}, R. Yakabe⁶⁹, D. Yamaguchi¹⁵⁸, Y. Yamaguchi¹¹⁹, A. Yamamoto⁶⁸, S. Yamamoto¹⁵⁶, T. Yamanaka¹⁵⁶, K. Yamauchi¹⁰⁴, Y. Yamazaki⁶⁹, Z. Yan²⁴, H. Yang^{35e}, H. Yang¹⁷³, Y. Yang¹⁵², Z. Yang¹⁵, W-M. Yao¹⁶, Y.C. Yap⁸², Y. Yasu⁶⁸, E. Yatsenko⁵, K.H. Yau Wong²³, J. Ye⁴², S. Ye²⁷, I. Yeletsikh⁶⁷, A.L. Yen⁵⁹, E. Yildirim⁸⁵, K. Yorita¹⁷¹, R. Yoshida⁶, K. Yoshihara¹²³, C. Young¹⁴⁴, C.J.S. Young³², S. Youssef²⁴, D.R. Yu¹⁶, J. Yu⁸, J.M. Yu⁹¹, J. Yu⁶⁶, L. Yuan⁶⁹, S.P.Y. Yuen²³, I. Yusuff^{30,44}, B. Zabinski⁴¹, R. Zaidan^{35d}, A.M. Zaitsev^{131,30}, N. Zakharchuk⁴⁴, J. Zalieckas¹⁵, A. Zaman¹⁴⁹, S. Zambito⁵⁹, L. Zanello^{133a,133b}, D. Zanzi⁹⁰, C. Zeitnitz¹⁷⁵, M. Zeman¹²⁹, A. Zemla^{40a}, J.C. Zeng¹⁶⁶, Q. Zeng¹⁴⁴, K. Zengel²⁵, O. Zenin¹³¹, T. Ženiš^{145a}, D. Zerwas¹¹⁸, D. Zhang⁹¹, F. Zhang¹⁷³, G. Zhang^{35b,39}, H. Zhang^{35c}, J. Zhang⁶, L. Zhang⁵⁰, R. Zhang²³, R. Zhang^{35b,45}, X. Zhang^{35d}, Z. Zhang¹¹⁸, X. Zhao⁴², Y. Zhao^{35d}, Z. Zhao^{35b}, A. Zhemchugov⁶⁷, J. Zhong¹²¹, B. Zhou⁹¹, C. Zhou⁴⁷, L. Zhou³⁷, L. Zhou⁴², M. Zhou¹⁴⁹, N. Zhou^{35f}, C.G. Zhu^{35d}, H. Zhu^{35a}, J. Zhu⁹¹, Y. Zhu^{35b}, X. Zhuang^{35a}, K. Zhukov⁹⁷, A. Zibell¹⁷⁴, D. Zieminska⁶³, N.I. Zimine⁶⁷, C. Zimmermann⁸⁵, S. Zimmermann⁵⁰, Z. Zinonos⁵⁶, M. Zinser⁸⁵, M. Ziolkowski¹⁴², L. Živković¹⁴, G. Zobernig¹⁷³, A. Zoccoli^{22a,22b}, M. zur Nedden¹⁷, L. Zwalinski³²

¹ Department of Physics, University of Adelaide, Adelaide, Australia

² Physics Department, SUNY Albany, Albany NY, United States

³ Department of Physics, University of Alberta, Edmonton AB, Canada

⁴ (a) Department of Physics, Ankara University, Ankara; (b) Istanbul Aydin University, Istanbul; (c) Division of Physics, TOBB University of Economics and Technology, Ankara, Turkey

⁵ LAPP, CNRS/IN2P3 and Université Savoie Mont Blanc, Annecy-le-Vieux, France

⁶ High Energy Physics Division, Argonne National Laboratory, Argonne IL, United States

⁷ Department of Physics, University of Arizona, Tucson AZ, United States

⁸ Department of Physics, The University of Texas at Arlington, Arlington TX, United States

⁹ Physics Department, University of Athens, Athens, Greece

¹⁰ Physics Department, National Technical University of Athens, Zografou, Greece

¹¹ Department of Physics, The University of Texas at Austin, Austin TX, United States

¹² Institute of Physics, Azerbaijan Academy of Sciences, Baku, Azerbaijan

¹³ Institut de Física d'Altes Energies (IFAE), The Barcelona Institute of Science and Technology, Barcelona, Spain

¹⁴ Institute of Physics, University of Belgrade, Belgrade, Serbia

¹⁵ Department for Physics and Technology, University of Bergen, Bergen, Norway

¹⁶ Physics Division, Lawrence Berkeley National Laboratory and University of California, Berkeley CA, United States

¹⁷ Department of Physics, Humboldt University, Berlin, Germany

¹⁸ Albert Einstein Center for Fundamental Physics and Laboratory for High Energy Physics, University of Bern, Bern, Switzerland

¹⁹ School of Physics and Astronomy, University of Birmingham, Birmingham, United Kingdom

²⁰ (a) Department of Physics, Bogazici University, Istanbul; (b) Department of Physics Engineering, Gaziantep University, Gaziantep; (d) Istanbul Bilgi University, Faculty of Engineering and Natural Sciences, Istanbul; (e) Bahcesehir University, Faculty of Engineering and Natural Sciences, Istanbul, Turkey

²¹ Centro de Investigaciones, Universidad Antonio Narino, Bogota, Colombia

²² (a) INFN Sezione di Bologna; (b) Dipartimento di Fisica e Astronomia, Università di Bologna, Bologna, Italy

²³ Physikalisches Institut, University of Bonn, Bonn, Germany

- ²⁴ Department of Physics, Boston University, Boston MA, United States
- ²⁵ Department of Physics, Brandeis University, Waltham MA, United States
- ²⁶ (a) Universidade Federal do Rio De Janeiro COPPE/EE/IF, Rio de Janeiro; (b) Electrical Circuits Department, Federal University of Juiz de Fora (UFJF), Juiz de Fora; (c) Federal University of Sao Joao del Rei (UFSJ), Sao Joao del Rei; (d) Instituto de Fisica, Universidade de Sao Paulo, Sao Paulo, Brazil
- ²⁷ Physics Department, Brookhaven National Laboratory, Upton NY, United States
- ²⁸ (a) Transilvania University of Brasov, Brasov, Romania; (b) National Institute of Physics and Nuclear Engineering, Bucharest; (c) National Institute for Research and Development of Isotopic and Molecular Technologies, Physics Department, Cluj Napoca; (d) University Politehnica Bucharest, Bucharest; (e) West University in Timisoara, Timisoara, Romania
- ²⁹ Departamento de Fisica, Universidad de Buenos Aires, Buenos Aires, Argentina
- ³⁰ Cavendish Laboratory, University of Cambridge, Cambridge, United Kingdom
- ³¹ Department of Physics, Carleton University, Ottawa ON, Canada
- ³² CERN, Geneva, Switzerland
- ³³ Enrico Fermi Institute, University of Chicago, Chicago IL, United States
- ³⁴ (a) Departamento de Fisica, Pontificia Universidad Católica de Chile, Santiago; (b) Departamento de Fisica, Universidad Técnica Federico Santa María, Valparaíso, Chile
- ³⁵ (a) Institute of High Energy Physics, Chinese Academy of Sciences, Beijing; (b) Department of Modern Physics, University of Science and Technology of China, Anhui; (c) Department of Physics, Nanjing University, Jiangsu; (d) School of Physics, Shandong University, Shandong; (e) Department of Physics and Astronomy, Shanghai Key Laboratory for Particle Physics and Cosmology, Shanghai Jiao Tong University, Shanghai⁴⁶; (f) Physics Department, Tsinghua University, Beijing 100084, China
- ³⁶ Laboratoire de Physique Corpusculaire, Clermont Université and Université Blaise Pascal and CNRS/IN2P3, Clermont-Ferrand, France
- ³⁷ Nevis Laboratory, Columbia University, Irvington NY, United States
- ³⁸ Niels Bohr Institute, University of Copenhagen, Copenhagen, Denmark
- ³⁹ (a) INFN Gruppo Collegato di Cosenza, Laboratori Nazionali di Frascati; (b) Dipartimento di Fisica, Università della Calabria, Rende, Italy
- ⁴⁰ (a) AGH University of Science and Technology, Faculty of Physics and Applied Computer Science, Krakow; (b) Marian Smoluchowski Institute of Physics, Jagiellonian University, Krakow, Poland
- ⁴¹ Institute of Nuclear Physics Polish Academy of Sciences, Krakow, Poland
- ⁴² Physics Department, Southern Methodist University, Dallas TX, United States
- ⁴³ Physics Department, University of Texas at Dallas, Richardson TX, United States
- ⁴⁴ DESY, Hamburg and Zeuthen, Germany
- ⁴⁵ Lehrstuhl für Experimentelle Physik IV, Technische Universität Dortmund, Dortmund, Germany
- ⁴⁶ Institut für Kern- und Teilchenphysik, Technische Universität Dresden, Dresden, Germany
- ⁴⁷ Department of Physics, Duke University, Durham NC, United States
- ⁴⁸ SUPA – School of Physics and Astronomy, University of Edinburgh, Edinburgh, United Kingdom
- ⁴⁹ INFN Laboratori Nazionali di Frascati, Frascati, Italy
- ⁵⁰ Fakultät für Mathematik und Physik, Albert-Ludwigs-Universität, Freiburg, Germany
- ⁵¹ Section de Physique, Université de Genève, Geneva, Switzerland
- ⁵² (a) INFN Sezione di Genova; (b) Dipartimento di Fisica, Università di Genova, Genova, Italy
- ⁵³ (a) E. Andronikashvili Institute of Physics, Iv. Javakhishvili Tbilisi State University, Tbilisi; (b) High Energy Physics Institute, Tbilisi State University, Tbilisi, Georgia
- ⁵⁴ II Physikalisches Institut, Justus-Liebig-Universität Giessen, Giessen, Germany
- ⁵⁵ SUPA – School of Physics and Astronomy, University of Glasgow, Glasgow, United Kingdom
- ⁵⁶ II Physikalisches Institut, Georg-August-Universität, Göttingen, Germany
- ⁵⁷ Laboratoire de Physique Subatomique et de Cosmologie, Université Grenoble-Alpes, CNRS/IN2P3, Grenoble, France
- ⁵⁸ Department of Physics, Hampton University, Hampton VA, United States
- ⁵⁹ Laboratory for Particle Physics and Cosmology, Harvard University, Cambridge MA, United States
- ⁶⁰ (a) Kirchhoff-Institut für Physik, Ruprecht-Karls-Universität Heidelberg, Heidelberg; (b) Physikalisches Institut, Ruprecht-Karls-Universität Heidelberg, Heidelberg; (c) ZITI Institut für technische Informatik, Ruprecht-Karls-Universität Heidelberg, Mannheim, Germany
- ⁶¹ Faculty of Applied Information Science, Hiroshima Institute of Technology, Hiroshima, Japan
- ⁶² (a) Department of Physics, The Chinese University of Hong Kong, Shatin, N.T., Hong Kong; (b) Department of Physics, The University of Hong Kong, Hong Kong; (c) Department of Physics, The Hong Kong University of Science and Technology, Clear Water Bay, Kowloon, Hong Kong, China
- ⁶³ Department of Physics, Indiana University, Bloomington IN, United States
- ⁶⁴ Institut für Astro- und Teilchenphysik, Leopold-Franzens-Universität, Innsbruck, Austria
- ⁶⁵ University of Iowa, Iowa City IA, United States
- ⁶⁶ Department of Physics and Astronomy, Iowa State University, Ames IA, United States
- ⁶⁷ Joint Institute for Nuclear Research, JINR Dubna, Dubna, Russia
- ⁶⁸ KEK, High Energy Accelerator Research Organization, Tsukuba, Japan
- ⁶⁹ Graduate School of Science, Kobe University, Kobe, Japan
- ⁷⁰ Faculty of Science, Kyoto University, Kyoto, Japan
- ⁷¹ Kyoto University of Education, Kyoto, Japan
- ⁷² Department of Physics, Kyushu University, Fukuoka, Japan
- ⁷³ Instituto de Fisica La Plata, Universidad Nacional de La Plata and CONICET, La Plata, Argentina
- ⁷⁴ Physics Department, Lancaster University, Lancaster, United Kingdom
- ⁷⁵ (a) INFN Sezione di Lecce; (b) Dipartimento di Matematica e Fisica, Università del Salento, Lecce, Italy
- ⁷⁶ Oliver Lodge Laboratory, University of Liverpool, Liverpool, United Kingdom
- ⁷⁷ Department of Physics, Jožef Stefan Institute and University of Ljubljana, Ljubljana, Slovenia
- ⁷⁸ School of Physics and Astronomy, Queen Mary University of London, London, United Kingdom
- ⁷⁹ Department of Physics, Royal Holloway University of London, Surrey, United Kingdom
- ⁸⁰ Department of Physics and Astronomy, University College London, London, United Kingdom
- ⁸¹ Louisiana Tech University, Ruston LA, United States
- ⁸² Laboratoire de Physique Nucléaire et de Hautes Energies, UPMC and Université Paris-Diderot and CNRS/IN2P3, Paris, France
- ⁸³ Fysiska institutionen, Lunds universitet, Lund, Sweden
- ⁸⁴ Departamento de Fisica Teorica C-15, Universidad Autonoma de Madrid, Madrid, Spain
- ⁸⁵ Institut für Physik, Universität Mainz, Mainz, Germany
- ⁸⁶ School of Physics and Astronomy, University of Manchester, Manchester, United Kingdom
- ⁸⁷ CPPM, Aix-Marseille Université and CNRS/IN2P3, Marseille, France
- ⁸⁸ Department of Physics, University of Massachusetts, Amherst MA, United States
- ⁸⁹ Department of Physics, McGill University, Montreal QC, Canada
- ⁹⁰ School of Physics, University of Melbourne, Victoria, Australia
- ⁹¹ Department of Physics, The University of Michigan, Ann Arbor MI, United States
- ⁹² Department of Physics and Astronomy, Michigan State University, East Lansing MI, United States
- ⁹³ (a) INFN Sezione di Milano; (b) Dipartimento di Fisica, Università di Milano, Milano, Italy
- ⁹⁴ B.I. Stepanov Institute of Physics, National Academy of Sciences of Belarus, Minsk, Belarus
- ⁹⁵ National Scientific and Educational Centre for Particle and High Energy Physics, Minsk, Belarus

- ⁹⁶ Group of Particle Physics, University of Montreal, Montreal QC, Canada
- ⁹⁷ P.N. Lebedev Physical Institute of the Russian Academy of Sciences, Moscow, Russia
- ⁹⁸ Institute for Theoretical and Experimental Physics (ITEP), Moscow, Russia
- ⁹⁹ National Research Nuclear University MEPhI, Moscow, Russia
- ¹⁰⁰ D.V. Skobeltsyn Institute of Nuclear Physics, M.V. Lomonosov Moscow State University, Moscow, Russia
- ¹⁰¹ Fakultät für Physik, Ludwig-Maximilians-Universität München, München, Germany
- ¹⁰² Max-Planck-Institut für Physik (Werner-Heisenberg-Institut), München, Germany
- ¹⁰³ Nagasaki Institute of Applied Science, Nagasaki, Japan
- ¹⁰⁴ Graduate School of Science and Kobayashi-Maskawa Institute, Nagoya University, Nagoya, Japan
- ¹⁰⁵ ^(a) INFN Sezione di Napoli; ^(b) Dipartimento di Fisica, Università di Napoli, Napoli, Italy
- ¹⁰⁶ Department of Physics and Astronomy, University of New Mexico, Albuquerque NM, United States
- ¹⁰⁷ Institute for Mathematics, Astrophysics and Particle Physics, Radboud University Nijmegen/Nikhef, Nijmegen, Netherlands
- ¹⁰⁸ Nikhef National Institute for Subatomic Physics and University of Amsterdam, Amsterdam, Netherlands
- ¹⁰⁹ Department of Physics, Northern Illinois University, DeKalb IL, United States
- ¹¹⁰ Budker Institute of Nuclear Physics, SB RAS, Novosibirsk, Russia
- ¹¹¹ Department of Physics, New York University, New York NY, United States
- ¹¹² Ohio State University, Columbus OH, United States
- ¹¹³ Faculty of Science, Okayama University, Okayama, Japan
- ¹¹⁴ Homer L. Dodge Department of Physics and Astronomy, University of Oklahoma, Norman OK, United States
- ¹¹⁵ Department of Physics, Oklahoma State University, Stillwater OK, United States
- ¹¹⁶ Palacký University, RCPM, Olomouc, Czech Republic
- ¹¹⁷ Center for High Energy Physics, University of Oregon, Eugene OR, United States
- ¹¹⁸ LAL, Univ. Paris-Sud, CNRS/IN2P3, Université Paris-Saclay, Orsay, France
- ¹¹⁹ Graduate School of Science, Osaka University, Osaka, Japan
- ¹²⁰ Department of Physics, University of Oslo, Oslo, Norway
- ¹²¹ Department of Physics, Oxford University, Oxford, United Kingdom
- ¹²² ^(a) INFN Sezione di Pavia; ^(b) Dipartimento di Fisica, Università di Pavia, Pavia, Italy
- ¹²³ Department of Physics, University of Pennsylvania, Philadelphia PA, United States
- ¹²⁴ National Research Centre "Kurchatov Institute" B.P. Konstantinov Petersburg Nuclear Physics Institute, St. Petersburg, Russia
- ¹²⁵ ^(a) INFN Sezione di Pisa; ^(b) Dipartimento di Fisica E. Fermi, Università di Pisa, Pisa, Italy
- ¹²⁶ Department of Physics and Astronomy, University of Pittsburgh, Pittsburgh PA, United States
- ¹²⁷ ^(a) Laboratório de Instrumentação e Física Experimental de Partículas – LIP, Lisboa; ^(b) Faculdade de Ciências, Universidade de Lisboa, Lisboa; ^(c) Department of Physics, University of Coimbra, Coimbra; ^(d) Centro de Física Nuclear da Universidade de Lisboa, Lisboa; ^(e) Departamento de Física, Universidade do Minho, Braga; ^(f) Departamento de Física Teórica y del Cosmos and CAFPE, Universidad de Granada, Granada (Spain); ^(g) Dep Física and CEFITEC de Faculdade de Ciências e Tecnologia, Universidade Nova de Lisboa, Caparica, Portugal
- ¹²⁸ Institute of Physics, Academy of Sciences of the Czech Republic, Praha, Czech Republic
- ¹²⁹ Czech Technical University in Prague, Praha, Czech Republic
- ¹³⁰ Faculty of Mathematics and Physics, Charles University in Prague, Praha, Czech Republic
- ¹³¹ State Research Center Institute for High Energy Physics (Protvino), NRC KI, Russia
- ¹³² Particle Physics Department, Rutherford Appleton Laboratory, Didcot, United Kingdom
- ¹³³ ^(a) INFN Sezione di Roma; ^(b) Dipartimento di Fisica, Sapienza Università di Roma, Roma, Italy
- ¹³⁴ ^(a) INFN Sezione di Roma Tor Vergata; ^(b) Dipartimento di Fisica, Università di Roma Tor Vergata, Roma, Italy
- ¹³⁵ ^(a) INFN Sezione di Roma Tre; ^(b) Dipartimento di Matematica e Fisica, Università Roma Tre, Roma, Italy
- ¹³⁶ ^(a) Faculté des Sciences Ain Chock, Réseau Universitaire de Physique des Hautes Energies – Université Hassan II, Casablanca; ^(b) Centre National de l'Energie des Sciences Techniques Nucleaires, Rabat; ^(c) Faculté des Sciences Semlalia, Université Cadi Ayyad, LPHEA-Marrakech; ^(d) Faculté des Sciences, Université Mohamed Premier and LPTPM, Oujda; ^(e) Faculté des sciences, Université Mohammed V, Rabat, Morocco
- ¹³⁷ DSM/IRFU (Institut de Recherches sur les Lois Fondamentales de l'Univers), CEA Saclay (Commissariat à l'Energie Atomique et aux Energies Alternatives), Gif-sur-Yvette, France
- ¹³⁸ Santa Cruz Institute for Particle Physics, University of California Santa Cruz, Santa Cruz CA, United States
- ¹³⁹ Department of Physics, University of Washington, Seattle WA, United States
- ¹⁴⁰ Department of Physics and Astronomy, University of Sheffield, Sheffield, United Kingdom
- ¹⁴¹ Department of Physics, Shinshu University, Nagano, Japan
- ¹⁴² Fachbereich Physik, Universität Siegen, Siegen, Germany
- ¹⁴³ Department of Physics, Simon Fraser University, Burnaby BC, Canada
- ¹⁴⁴ SLAC National Accelerator Laboratory, Stanford CA, United States
- ¹⁴⁵ ^(a) Faculty of Mathematics, Physics & Informatics, Comenius University, Bratislava; ^(b) Department of Subnuclear Physics, Institute of Experimental Physics of the Slovak Academy of Sciences, Kosice, Slovak Republic
- ¹⁴⁶ ^(a) Department of Physics, University of Cape Town, Cape Town; ^(b) Department of Physics, University of Johannesburg, Johannesburg; ^(c) School of Physics, University of the Witwatersrand, Johannesburg, South Africa
- ¹⁴⁷ ^(a) Department of Physics, Stockholm University; ^(b) The Oskar Klein Centre, Stockholm, Sweden
- ¹⁴⁸ Physics Department, Royal Institute of Technology, Stockholm, Sweden
- ¹⁴⁹ Departments of Physics & Astronomy and Chemistry, Stony Brook University, Stony Brook NY, United States
- ¹⁵⁰ Department of Physics and Astronomy, University of Sussex, Brighton, United Kingdom
- ¹⁵¹ School of Physics, University of Sydney, Sydney, Australia
- ¹⁵² Institute of Physics, Academia Sinica, Taipei, Taiwan
- ¹⁵³ Department of Physics, Technion: Israel Institute of Technology, Haifa, Israel
- ¹⁵⁴ Raymond and Beverly Sackler School of Physics and Astronomy, Tel Aviv University, Tel Aviv, Israel
- ¹⁵⁵ Department of Physics, Aristotle University of Thessaloniki, Thessaloniki, Greece
- ¹⁵⁶ International Center for Elementary Particle Physics and Department of Physics, The University of Tokyo, Tokyo, Japan
- ¹⁵⁷ Graduate School of Science and Technology, Tokyo Metropolitan University, Tokyo, Japan
- ¹⁵⁸ Department of Physics, Tokyo Institute of Technology, Tokyo, Japan
- ¹⁵⁹ Department of Physics, University of Toronto, Toronto ON, Canada
- ¹⁶⁰ ^(a) TRIUMF, Vancouver BC; ^(b) Department of Physics and Astronomy, York University, Toronto ON, Canada
- ¹⁶¹ Faculty of Pure and Applied Sciences, and Center for Integrated Research in Fundamental Science and Engineering, University of Tsukuba, Tsukuba, Japan
- ¹⁶² Department of Physics and Astronomy, Tufts University, Medford MA, United States
- ¹⁶³ Department of Physics and Astronomy, University of California Irvine, Irvine CA, United States
- ¹⁶⁴ ^(a) INFN Gruppo Collegato di Udine, Sezione di Trieste, Udine; ^(b) ICTP, Trieste; ^(c) Dipartimento di Chimica, Fisica e Ambiente, Università di Udine, Udine, Italy
- ¹⁶⁵ Department of Physics and Astronomy, University of Uppsala, Uppsala, Sweden
- ¹⁶⁶ Department of Physics, University of Illinois, Urbana IL, United States
- ¹⁶⁷ Instituto de Física Corpuscular (IFIC) and Departamento de Física Atomica, Molecular y Nuclear and Departamento de Ingeniería Electrónica and Instituto de Microelectrónica de Barcelona (IMB-CNM), University of Valencia and CSIC, Valencia, Spain

- ¹⁶⁸ Department of Physics, University of British Columbia, Vancouver BC, Canada
- ¹⁶⁹ Department of Physics and Astronomy, University of Victoria, Victoria BC, Canada
- ¹⁷⁰ Department of Physics, University of Warwick, Coventry, United Kingdom
- ¹⁷¹ Waseda University, Tokyo, Japan
- ¹⁷² Department of Particle Physics, The Weizmann Institute of Science, Rehovot, Israel
- ¹⁷³ Department of Physics, University of Wisconsin, Madison WI, United States
- ¹⁷⁴ Fakultät für Physik und Astronomie, Julius-Maximilians-Universität, Würzburg, Germany
- ¹⁷⁵ Fakultät für Mathematik und Naturwissenschaften, Fachgruppe Physik, Bergische Universität Wuppertal, Wuppertal, Germany
- ¹⁷⁶ Department of Physics, Yale University, New Haven CT, United States
- ¹⁷⁷ Yerevan Physics Institute, Yerevan, Armenia
- ¹⁷⁸ Centre de Calcul de l'Institut National de Physique Nucléaire et de Physique des Particules (IN2P3), Villeurbanne, France

- ¹ Also at Department of Physics, King's College London, London, United Kingdom.
- ² Also at Institute of Physics, Azerbaijan Academy of Sciences, Baku, Azerbaijan.
- ³ Also at Novosibirsk State University, Novosibirsk, Russia.
- ⁴ Also at TRIUMF, Vancouver BC, Canada.
- ⁵ Also at Department of Physics & Astronomy, University of Louisville, Louisville, KY, United States of America.
- ⁶ Also at Department of Physics, California State University, Fresno CA, United States of America.
- ⁷ Also at Department of Physics, University of Fribourg, Fribourg, Switzerland.
- ⁸ Also at Departament de Física de la Universitat Autònoma de Barcelona, Barcelona, Spain.
- ⁹ Also at Departamento de Física e Astronomia, Faculdade de Ciências, Universidade do Porto, Portugal.
- ¹⁰ Also at Tomsk State University, Tomsk, Russia.
- ¹¹ Also at Università di Napoli Parthenope, Napoli, Italy.
- ¹² Also at Institute of Particle Physics (IPP), Canada.
- ¹³ Also at National Institute of Physics and Nuclear Engineering, Bucharest, Romania.
- ¹⁴ Also at Department of Physics, St. Petersburg State Polytechnical University, St. Petersburg, Russia.
- ¹⁵ Also at Department of Physics, The University of Michigan, Ann Arbor MI, United States of America.
- ¹⁶ Also at Centre for High Performance Computing, CSIR Campus, Rosebank, Cape Town, South Africa.
- ¹⁷ Also at Louisiana Tech University, Ruston LA, United States of America.
- ¹⁸ Also at Institutio Catalana de Recerca i Estudis Avançats, ICREA, Barcelona, Spain.
- ¹⁹ Also at Graduate School of Science, Osaka University, Osaka, Japan.
- ²⁰ Also at Department of Physics, National Tsing Hua University, Taiwan.
- ²¹ Also at Institute for Mathematics, Astrophysics and Particle Physics, Radboud University Nijmegen/Nikhef, Nijmegen, Netherlands.
- ²² Also at Department of Physics, The University of Texas at Austin, Austin TX, United States of America.
- ²³ Also at CERN, Geneva, Switzerland.
- ²⁴ Also at Georgian Technical University (GTU), Tbilisi, Georgia.
- ²⁵ Also at O Chadai Academic Production, Ochanomizu University, Tokyo, Japan.
- ²⁶ Also at Manhattan College, New York NY, United States of America.
- ²⁷ Also at Hellenic Open University, Patras, Greece.
- ²⁸ Also at Academia Sinica Grid Computing, Institute of Physics, Academia Sinica, Taipei, Taiwan.
- ²⁹ Also at School of Physics, Shandong University, Shandong, China.
- ³⁰ Also at Moscow Institute of Physics and Technology State University, Dolgoprudny, Russia.
- ³¹ Also at Section de Physique, Université de Genève, Geneva, Switzerland.
- ³² Also at Eotvos Lorand University, Budapest, Hungary.
- ³³ Also at Departments of Physics & Astronomy and Chemistry, Stony Brook University, Stony Brook NY, United States of America.
- ³⁴ Also at International School for Advanced Studies (SISSA), Trieste, Italy.
- ³⁵ Also at Department of Physics and Astronomy, University of South Carolina, Columbia SC, United States of America.
- ³⁶ Also at School of Physics and Engineering, Sun Yat-sen University, Guangzhou, China.
- ³⁷ Also at Institute for Nuclear Research and Nuclear Energy (INRNE) of the Bulgarian Academy of Sciences, Sofia, Bulgaria.
- ³⁸ Also at Faculty of Physics, M.V. Lomonosov Moscow State University, Moscow, Russia.
- ³⁹ Also at Institute of Physics, Academia Sinica, Taipei, Taiwan.
- ⁴⁰ Also at National Research Nuclear University MEPhI, Moscow, Russia.
- ⁴¹ Also at Department of Physics, Stanford University, Stanford CA, United States of America.
- ⁴² Also at Institute for Particle and Nuclear Physics, Wigner Research Centre for Physics, Budapest, Hungary.
- ⁴³ Also at Flensburg University of Applied Sciences, Flensburg, Germany.
- ⁴⁴ Also at University of Malaya, Department of Physics, Kuala Lumpur, Malaysia.
- ⁴⁵ Also at CPPM, Aix-Marseille Université and CNRS/IN2P3, Marseille, France.
- ⁴⁶ Also affiliated with PKU-CHEP.
- * Deceased.